

# Fenchel-Young Estimators of Perturbed Utility Models

Xi Lin<sup>a</sup>, Yafeng Yin<sup>a,b,\*</sup>, and Tianming Liu<sup>a</sup>

<sup>a</sup>*Department of Civil and Environmental Engineering, University of Michigan, Ann Arbor, MI 48109, USA*

<sup>b</sup>*Department of Industrial and Operations Engineering, University of Michigan, Ann Arbor, MI 48109, USA*

*\*Corresponding author.*

*Email addresses: xilina, yafeng, tianmliu@umich.edu .*

February 26, 2026

## Abstract

The Perturbed Utility Model framework offers a powerful generalization of discrete choice analysis, unifying models like Multinomial Logit and Sparsemax through convex optimization. However, standard Maximum Likelihood Estimation (MLE) faces severe theoretical and numerical challenges when applied to this broader class, particularly regarding non-convexity and instability in sparse regimes. To resolve these issues, this paper introduces a unified estimation framework based on the Fenchel-Young loss. By leveraging the intrinsic convex conjugate structure of PUMs, we demonstrate that the Fenchel-Young estimator guarantees global convexity and bounded gradients, providing a mathematically natural alternative to MLE.

Addressing the critical challenge of data scarcity, we further extend this framework via Wasserstein Distributionally Robust Optimization. We first derive an exact finite-dimensional reformulation of the infinite-dimensional primal problem, establishing its theoretical convexity. However, recognizing that the resulting worst-case constraints involve computationally intractable inner maximizations, we subsequently construct a tractable safe approximation by exploiting the global Lipschitz continuity of the Fenchel-Young loss. Through this tractable formulation, we uncover a rigorous geometric unification: two canonical regularization techniques—standard  $\ell_2$ -regularization and the margin-enforcing Hinge loss—emerge mathematically as specific limiting cases of our distributionally robust estimator. Extensive experiments on synthetic data and the Swissmetro benchmark validate that the proposed framework significantly outperforms traditional methods, recovering stable preferences even under severe data limitations.

## 1 Introduction

Since the seminal contributions of Daniel McFadden established the econometrics of discrete choice (McFadden, 1972), this framework has become the dominant paradigm for analyzing decision-making behavior across a wide range of fields, including transportation (McFadden, 1974; Ben-Akiva and Lerman, 1985), marketing (Malhotra, 1984) and health economics (Clark et al., 2014). Within this paradigm, individuals are assumed to select alternatives so as to maximize utility subject to stochastic perturbations, giving rise to the Random Utility Model (RUM). Among its many operationalizations, the Multinomial Logit (MNL) model has emerged as the canonical baseline due to its analytical tractability and closed-form probability representation (Hausman and McFadden, 1984). In addition, the MNL model possesses a profound computational elegance: estimating its parameters from data via Maximum Likelihood Estimation (MLE; Wald, 1949) constitutes a globally convex optimization problem (Donoso and de Grange, 2010). This convexity ensures uniqueness of the estimator and

numerical stability independent of initialization, rendering inference both theoretically well-posed and computationally efficient. The alignment between behavioral microfoundations and convex optimization geometry has therefore cemented the MNL–MLE framework as the classical foundation for the inverse recovery of agent preferences from observed choice data.

Despite its foundational role, this classical RUM framework exhibits well-documented structural limitations. Most notably, the Independence of Irrelevant Alternatives (IIA) property imposes restrictive substitution patterns (Ray, 1973), while the reliance on specific distributional assumptions for stochastic errors constrains behavioral flexibility. These limitations have motivated a rich body of extensions, including Probit (Daganzo et al., 1977) and Nested Logit formulations (Wen and Koppelman, 2001), which relax distributional and correlation constraints at the cost of increased computational complexity.

More recently, discrete choice theory has undergone a conceptual generalization through the Perturbed Utility Model (PUM) framework (McFadden and Fosgerau, 2012; Fudenberg et al., 2015). Rather than deriving choice probabilities from exogenously specified stochastic error distributions, the PUM framework formulates decision-making as utility maximization under a convex perturbation (or regularization) functional defined over the probability simplex. Formally, the decision-maker selects a probability vector that maximizes expected utility net of a convex penalty capturing information-processing costs, bounded rationality, or intrinsic preference for randomization.

Central to this framework is the duality between the perturbation function and the surplus (expected maximum utility) function. Building on McFadden’s surplus theory (McFadden, 1981), the expected maximum perturbed utility defines a convex potential whose gradient yields the choice probabilities. Through Legendre–Fenchel duality (Touchette, 2005; McFadden and Fosgerau, 2012), any admissible discrete choice model can thus be generated from a convex perturbation function, establishing a one-to-one correspondence between stochastic choice behavior and convex regularization structures. Classical models are recovered as special cases; for example, the MNL model arises when the perturbation corresponds to negative Shannon entropy (Anderson et al., 1992)

This convex-analytic perspective reveals discrete choice models as points within a broader geometric space of decision mechanisms. It also clarifies the equivalence between additive random utility formulations and regularized optimization representations, a connection that has been operationalized in evolutionary game dynamics and stochastic learning models through smooth best-response mappings (Hofbauer and Sandholm, 2002). Complementarily, revealed-preference foundations for perturbed utility have been established by Fudenberg et al. (2015), who provide axiomatic conditions under which stochastic choice data admit a convex perturbation representation.

Owing to its structural generality and analytical tractability, the PUM framework has begun to permeate transportation science and related fields. It has proven particularly valuable in stochastic route choice modeling and entropy-regularized traffic assignment, where convex potential structures facilitate equilibrium analysis and computational scalability (Fosgerau et al., 2022; Yao et al., 2024). More broadly, the framework provides a unifying language for integrating behavioral realism, information frictions, and optimization geometry within a single modeling architecture.

Given the structural elegance of the PUM framework as a generalization of classical discrete choice, a fundamental question arises regarding its statistical inference: how can the parameters of a general PUM be reliably estimated from observed choice data? The most immediate strategy is to extend the classical MLE paradigm, which serves as the gold standard for MNL estimation. In the specific case of the logit model, the negative log-likelihood is globally convex with respect to the utility parameters, ensuring tractable optimization and statistically efficient estimators.

However, these desirable properties do not automatically generalize to arbitrary perturbations. The convex geometry induced by entropic regularization is highly specific; alternative perturbation

structures may violate log-concavity, rendering the likelihood non-convex. More critically, many modern PUM specifications induce sparse choice probabilities. Unlike the MNL model, which assigns strictly positive probability to all alternatives (dense support), perturbations such as the quadratic regularization (e.g., Sparsemax; Martins and Astudillo, 2016; Gabaix, 2014) frequently yield corner solutions with strictly zero probabilities for low-utility alternatives. In such regimes, the standard MLE objective fails catastrophically; the logarithm of a zero probability diverges to negative infinity, rendering the loss function undefined and the optimization numerically unstable. This structural incompatibility suggests that likelihood geometry is misaligned with the broader convex structure of PUMs.

Beyond the geometrical challenges of estimation, a parallel statistical hurdle persists: data scarcity. Paradoxically, despite the pervasive narrative of a big data era, practical applications of discrete choice modeling frequently encounter severe limitations in sample size. Constraints such as high survey costs, limited sensor deployment, and stringent privacy regulations often force analysts to rely on small datasets. In the same-sample regimes, MNL estimators are known to exhibit finite-sample bias and overfitting tendencies (Albert and Anderson, 1984; Firth, 1993; Sur and Candès, 2019). These vulnerabilities are amplified in flexible PUM specifications, where high-dimensional perturbation structures exacerbate statistical instability.

In this paper, we develop a unified estimation framework for PUMs grounded in Fenchel–Young loss functions (Blondel et al., 2019, 2020). Exploiting the intrinsic convex conjugacy that defines the PUM architecture, we show that the Fenchel–Young estimator constitutes the most natural scoring rule for this class of models. By aligning the geometry of the loss function with the convex structure of the surplus function, we prove that the Fenchel-Young estimator yields a globally convex optimization problem for any admissible PUM, even those inducing sparse probabilities, while maintaining desirable asymptotic statistical properties.

To address the critical challenge of estimation in data-scarce regimes, we extend this framework by incorporating Wasserstein Distributionally Robust Optimization (DRO; Mohajerin Esfahani and Kuhn, 2018; Kuhn et al., 2019; Gao and Kleywegt, 2023). We construct a Wasserstein ambiguity set around the empirical distribution to explicitly immunize the estimator against the finite-sample bias and overfitting risks inherent to small datasets. Crucially, we first derive an exact finite-dimensional reformulation of the worst-case problem, proving that it preserves the underlying convexity of the nominal Fenchel-Young objective. However, acknowledging that the exact constraints involve computationally prohibitive inner maximizations, we subsequently develop a tractable safe approximation by leveraging the Lipschitz continuity of the loss function. This yields a computationally efficient convex program solvable via standard duality-based techniques.

A notable byproduct of this robustification is the emergence of a unifying geometric interpretation: the classical  $\ell_2$  regularization and the Hinge loss arise as limiting cases of our approximate Wasserstein Fenchel-Young estimator under specific ambiguity set configurations.

The remainder of this paper is organized as follows. Section 2 provides a rigorous characterization of the PUM framework for discrete choice, establishing the foundational link between convex perturbation functions and choice probability generation. In Section 3, we introduce the Fenchel-Young estimator, analyzing its global convexity and asymptotic properties as a mathematically natural alternative to MLE. Section 4 addresses the challenge of estimation under data scarcity by developing the Wasserstein DRO framework. Here, we derive the tractable dual reformulations and establish the theoretical connections to  $\ell_2$  regularization and the Hinge loss. Section 5 presents comprehensive numerical experiments on both synthetic datasets and the Swissmetro dataset (Bierlaire et al., 2001) to validate the robustness and efficiency of the proposed methods. Finally, Section 6 concludes the paper.

## 2 Perturbed Utility Models

### 2.1 Basics and Examples

In this subsection, we provide a characterization of the PUM framework as established by McFadden and Fosgerau (2012) and Fudenberg et al. (2015), which derives choice probabilities through a convex optimization principle. This perspective is particularly advantageous for the upcoming Fenchel-Young estimation as it exposes the geometric structure of the choice probability mapping.

#### 2.1.1 The Primal Formulation: Utility Maximization with Regularization

Consider a decision-maker  $n$  facing a finite set of mutually exclusive alternatives  $\mathcal{C}$ . Let  $\mathbf{V}_n \in \mathbb{R}^{|\mathcal{C}|}$  denote the vector of systematic (deterministic) utilities, where  $V_{ni} = \boldsymbol{\beta}^\top \mathbf{x}_{ni}$  is the utility of alternative  $i \in \mathcal{C}$ ,  $\mathbf{x}_{ni}$  is a vector of observed attributes, and  $\boldsymbol{\beta}$  is the vector of unknown parameters to be estimated.

In the PUM framework, the decision-maker is assumed to maximize the expected systematic utility minus a convex penalty function that represents the cost of information processing or the intrinsic preference for randomization. Let  $\mathbf{p}_n \in \Delta$  be the choice probability vector, where  $\Delta = \{\mathbf{p} \in \mathbb{R}^{|\mathcal{C}|} \mid \mathbf{p} \geq 0, \sum_{i \in \mathcal{C}} p_i = 1\}$  is the probability simplex.

The choice probability vector  $\mathbf{p}_n$  is defined as the unique solution to the following convex optimization problem:

$$\mathbf{p}_n(\mathbf{V}_n) = \arg \max_{\mathbf{p} \in \Delta} \left\{ \sum_{i \in \mathcal{C}} p_i V_{ni} - \Lambda(\mathbf{p}) \right\}, \quad (1)$$

where  $\Lambda : \Delta \rightarrow \mathbb{R} \cup \{\infty\}$  is the *perturbation function* (or regularizer). We assume  $\Lambda$  satisfies the following standard regularity conditions:

- (A1)  $\Lambda$  is strictly convex on the relative interior of  $\Delta$ .
- (A2)  $\Lambda$  is continuously differentiable on the relative interior of  $\Delta$ .
- (A3) The gradient of  $\Lambda$  diverges at the boundary of  $\Delta$  (for models with full support) or admits a subgradient structure allowing for corner solutions.

#### 2.1.2 Convex Conjugacy and the Generalized Williams-Daly-Zachary Theorem

The structural properties of the PUM are best understood through Fenchel-Legendre duality. The convex conjugate of the perturbation function  $\Lambda(\mathbf{p})$ , typically interpreted as the *surplus function* or the *expected maximum utility*, is defined as:

$$\Omega(\mathbf{V}_n) = \sup_{\mathbf{p} \in \Delta} \left\{ \mathbf{p}^\top \mathbf{V}_n - \Lambda(\mathbf{p}) \right\}. \quad (2)$$

By the envelope theorem and the properties of convex conjugation, the relationship between the utility vector and the choice probability is given by the gradient of the surplus function. This yields a generalized version of the Williams-Daly-Zachary theorem:

**Proposition 1** (PUM Duality). *Under assumptions (A1)-(A2), the surplus function  $\Omega(\mathbf{V}_n)$  is convex and differentiable everywhere on  $\mathbb{R}^{|\mathcal{C}|}$ . Furthermore, the optimal choice probability vector satisfying Eq. (1) is given by:*

$$\mathbf{p}_n = \nabla_{\mathbf{V}} \Omega(\mathbf{V}_n). \quad (3)$$

This duality is central to our estimation strategy. It implies that estimating  $\beta$  amounts to choosing parameters so that the probability vectors generated by Eq.(3) align with observed choice realizations under an appropriate loss function.

### 2.1.3 Additive Separability and the Choice Kernel

A particularly tractable subclass of PUMs arises when the perturbation function  $\Lambda(\mathbf{p})$  decomposes into a sum of univariate convex functions (McFadden and Fosgerau, 2012). This structural assumption, known as *additive separability*, is satisfied by the majority of discrete choice models used in practice, including MNL and Sparsemax. Additive separability yields semi-analytical choice kernels, while still encompassing a broad class of non-logit and sparse choice models. Furthermore, we note that non-separable perturbations can encode richer cross-alternative interactions; although they typically lead to implicit choice mappings and intractable inference in conventional settings, our proposed framework successfully overcomes these computational hurdles to accommodate non-separable cases as well.

**Definition 1** (Additive Separable PUM). A PUM is said to be **additive separable** if the regularization function admits the form:

$$\Lambda(\mathbf{p}) = \sum_{i \in \mathcal{C}} h(p_i), \quad (4)$$

where  $h : [0, 1] \rightarrow \mathbb{R}$  is a strictly convex, continuously differentiable function.

For additive separable models, the complex interdependence between alternatives in the optimization problem (1) is decoupled. The first-order optimality conditions imply that for each alternative  $i$ , the relationship between the probability  $p_i$  and the utility  $V_i$  is mediated solely by a global normalization constant.

**Definition 2** (Choice Kernel). Let  $h(\cdot)$  be the component-wise convex regularizer. The **Choice Kernel**, denoted by  $\psi : \mathbb{R} \rightarrow [0, 1]$ , is defined as the inverse of the derivative of the regularizer:

$$\psi(z) \triangleq (h')^{-1}(z). \quad (5)$$

Note that, by the convexity of  $h(\cdot)$ , the choice kernel function  $\psi(\cdot)$  must be a monotone function. Using the choice kernel, the optimal choice probability for any alternative  $i$  takes the form:

$$p_i(\mathbf{V}) = \psi(V_i - \lambda(\mathbf{V})), \quad (6)$$

where  $\lambda(\mathbf{V})$  is the Lagrange multiplier associated with the simplex constraint  $\sum p_j = 1$ . The value of  $\lambda(\mathbf{V})$  is uniquely determined as the solution to the implicit equation:

$$\sum_{j \in \mathcal{C}} \psi(V_j - \lambda) = 1. \quad (7)$$

The choice kernel  $\psi$  characterizes the local response of the decision-maker to utility stimuli. It maps the effective utility (systematic utility  $V_i$  adjusted by the shadow price of the budget constraint  $\lambda$ ) directly to the choice probability.

### 2.1.4 Specific Instances

The PUM framework unifies various discrete choice specifications through the choice of  $\Lambda(\mathbf{p})$ .

**Multinomial Logit (MNL):** The standard MNL model is recovered when the perturbation function is the negative Shannon entropy scaled by a dispersion parameter  $\mu > 0$ :

$$\Lambda_{\text{Logit}}(\mathbf{p}) = \mu \sum_{i \in \mathcal{C}} p_i \ln p_i. \quad (8)$$

The corresponding conjugate function is the familiar Log-Sum-Exp function:

$$\Omega_{\text{Logit}}(\mathbf{V}) = \mu \ln \left( \sum_{i \in \mathcal{C}} \exp \left( \frac{V_i}{\mu} \right) \right). \quad (9)$$

**The Sparsemax Model (Quadratic Regularization):** A distinct and distinctively robust instance of the PUM arises when the entropic penalty is replaced by a quadratic Euclidean norm, scaled by a dispersion parameter  $\mu > 0$ . Specifically, let the regularization function be defined as the scaled squared  $\ell_2$ -norm:

$$\Lambda_{\text{Sparse}}(\mathbf{p}) = \frac{\mu}{2} \|\mathbf{p}\|_2^2. \quad (10)$$

Substituting this into the primal problem (1) reveals that the choice probability vector is the Euclidean projection of the *scaled* utility vector  $\mathbf{V}_n/\mu$  onto the probability simplex  $\Delta$ . Mathematically, this is equivalent to solving the minimum distance problem:

$$\mathbf{p}_n^{\text{Sparse}} = \arg \min_{\mathbf{p} \in \Delta} \left\| \mathbf{p} - \frac{\mathbf{V}_n}{\mu} \right\|_2^2. \quad (11)$$

Unlike the Multinomial Logit model, which yields strictly positive probabilities for all alternatives (dense support), the Sparsemax model admits a closed-form solution with *compact support*:

$$p_{ni} = \max \left\{ 0, \frac{V_{ni}}{\mu} - \lambda(\mathbf{V}_n, \mu) \right\}, \quad (12)$$

where  $\lambda(\mathbf{V}_n, \mu)$  is a threshold function determined effectively by the normalization constraint  $\sum p_{ni} = 1$ .

Here, the parameter  $\mu$  governs the sparsity of the decision: a smaller  $\mu$  amplifies the utility differences (similar to a lower temperature in Logit), pushing the projection towards the simplex vertices (hard-max), whereas a larger  $\mu$  shrinks the effective utilities towards zero, resulting in a more uniform and denser probability distribution.

**The Cauchy Model:** To capture behaviors with heavier tails than the Gumbel distribution (implied by MNL), one can employ a perturbation derived from the Cauchy distribution. The specific additive regularizer is given by:

$$\Lambda_{\text{Cauchy}}(\mathbf{p}) = -\frac{\mu}{\pi} \sum_{i \in \mathcal{C}} \ln \left( \cos \left( \pi \left( p_i - \frac{1}{2} \right) \right) \right). \quad (13)$$

This formulation corresponds to the cumulative distribution function of the standard Cauchy distribution. The explicit probability function is derived from the first-order optimality condition  $\nabla \Lambda(\mathbf{p}) = \mathbf{V} - \lambda \mathbf{1}$ . Specifically, differentiating the regularization term yields the tangent link function:

$$\frac{V_{ni} - \lambda}{\mu} = \tan \left( \pi \left( p_{ni} - \frac{1}{2} \right) \right). \quad (14)$$

Inverting this relationship gives the choice probability:

$$p_{ni} = \frac{1}{2} + \frac{1}{\pi} \arctan \left( \frac{V_{ni} - \lambda}{\mu} \right). \quad (15)$$

where  $\lambda$  ensures all probabilities sum up to 1.

Unlike MNL and Sparsemax, this model is generated by a heavy-tailed perturbation. This structural characteristic results in choice probabilities that decay polynomially rather than exponentially as utility decreases, maintaining a fatter tail than the standard MNL model. Consequently, the Cauchy specification is particularly effective for capturing noisy decision-making scenarios where agents retain a non-negligible likelihood of selecting low-utility alternatives, thereby accommodating significant deviations from strict utility maximization.

### 3 Fenchel-Young Estimation of Perturbed Utility Models

Having established the structural link between the utility vector and choice probabilities via the gradient of the surplus function, we now turn to the estimation of the model parameters. Let the dataset consist of  $N$  independent observations. For each decision-maker  $n$ , let  $\mathbf{x}_n$  denote the matrix of observed attributes, and let  $\mathbf{y}_n \in \{0, 1\}^{|\mathcal{C}|}$  denote the observed choice as a one-hot vector, where  $y_{ni} = 1$  if alternative  $i$  is chosen and 0 otherwise.

#### 3.1 The Pathologies of Maximum Likelihood Estimation

While MLE constitutes the standard approach for discrete choice analysis, its reliance on the logarithmic scoring rule proves structurally inadequate for the broader class of PUMs. This incompatibility manifests as two critical pathologies. First, in models with sparse choice kernels, the assignment of zero probability to an observed alternative triggers a mathematical singularity, causing the objective function to diverge to negative infinity. Second, even in regimes with full support, the negative log-likelihood generally fails to preserve global convexity for some perturbation functions, rendering the optimization landscape numerically unstable.

##### 3.1.1 The Zero-Probability Singularity

A fundamental theoretical distinction between the classical MNL and the broader class of PUMs lies in the geometry of the probability simplex. While the entropic perturbation of the MNL forces the solution into the relative interior of the simplex (ensuring  $p_{ni} > 0$  for all  $i$ ), modern PUM specifications such as Sparsemax are explicitly designed to yield corner solutions. In these sparse regimes, low-utility alternatives result in strictly zero probabilities.

This sparsity, while computationally and behaviorally desirable, renders the standard MLE structurally undefined. Consider the negative log-likelihood objective function for a dataset of  $N$  observations:

$$\mathcal{L}_{\text{NLL}}(\boldsymbol{\beta}) = - \sum_{n=1}^N \sum_{i \in \mathcal{C}} y_{ni} \ln(p_{ni}(\boldsymbol{\beta})), \quad (16)$$

where  $y_n$  denotes the index of the observed choice. Specifically, if the model predicts  $p_{n,y_n}(\boldsymbol{\beta}) = 0$  for even a single observation  $n$ , the loss function suffers a mathematical singularity:

$$\lim_{p \rightarrow 0^+} -\ln(p) = +\infty. \quad (17)$$

Consequently, the objective function becomes unbounded, and the gradient is undefined. This is not merely a numerical nuisance but a catastrophic failure of the estimator: the logarithmic geometry imposes an infinite penalty on “hard” mistakes, preventing the optimization algorithm from navigating the parameter space.

### 3.1.2 Non-Convexity

Beyond the numerical singularities encountered in sparse regimes, MLE faces a severe theoretical impediment even when applied to models with dense support. The reliance on the logarithmic scoring rule implies that the convexity of the estimation problem is not guaranteed for general perturbations, but rather contingent on specific tail behaviors. The negative log-likelihood loss for a PUM is given by  $\ell_{\text{NLL}}(\boldsymbol{\beta}) = -\ln p_y(\mathbf{V}(\boldsymbol{\beta}))$ . For this objective to be convex with respect to linear utility parameters  $\boldsymbol{\beta}$ , the choice probability map  $\mathbf{p}(\mathbf{V}) = \nabla\Omega(\mathbf{V})$  must be *log-concave*. While this condition holds for MNL (where probabilities are derived from the Gumbel distribution, which is log-concave), it fails for some models induced by heavy-tailed perturbations. Below we provide a concrete example.

**Example 1** (Non-convexity of MLE for Cauchy PUMs). Consider a binary choice model generated by a heavy-tailed perturbation, specifically one where the choice kernel  $\psi(\cdot)$  corresponds to the cumulative distribution function of the standard Cauchy distribution:

$$p_1(z) = \psi(z) = \frac{1}{2} + \frac{1}{\pi} \arctan(z), \quad z = V_1 - V_2. \quad (18)$$

Within the additive separable PUM framework, this kernel arises from a one-dimensional regularizer  $h : [0, 1] \rightarrow \mathbb{R}$  such that

$$\psi(z) = (h')^{-1}(z).$$

So we have

$$h(p) = -\frac{1}{\pi} \log \left( \cos \left( \pi \left( p - \frac{1}{2} \right) \right) \right) + C, \quad (19)$$

which is strictly convex on  $(0, 1)$ . The corresponding Cauchy PUM is then defined by the additive separable regularizer

$$\Lambda_{\text{Cauchy}}(\mathbf{p}) = \sum_{i \in \mathcal{C}} h(p_i) = -\frac{1}{\pi} \sum_{i \in \mathcal{C}} \log \left( \cos \left( \pi \left( p_i - \frac{1}{2} \right) \right) \right) + C', \quad \mathbf{p} \in \Delta. \quad (20)$$

Despite being a valid PUM generated by a strictly convex  $\Lambda_{\text{Cauchy}}$ , the induced choice probability  $p_1(z)$  is *not log-concave*. The second derivative of the negative log-likelihood with respect to  $z$ ,  $\frac{d^2}{dz^2}[-\ln \psi(z)]$ , becomes negative in the left tail (specifically for  $z < -\sqrt{3}$ ), indicating local non-convexity. Consequently, standard gradient-based MLE solvers may get trapped in local optima or diverge, whereas the Fenchel–Young estimator for the exact same model remains globally convex and tractable.

These structural failures necessitate a fundamental departure from the logarithmic scoring rule. Rather than forcing an ill-fitting geometry upon the model, we propose an estimation framework derived directly from the PUM’s intrinsic convex conjugate structure. This leads to the Fenchel–Young loss.

### 3.2 The Loss Function

To address the above problems, and to provide a unified convex optimization framework for all PUMs, we adopt the *Fenchel-Young Loss* (FYLoss) as our estimation objective. Leveraging the duality structure of PUMs, the loss for an observation  $(\mathbf{x}, \mathbf{y})$  is defined as:

$$\ell_{\text{FY}}(\boldsymbol{\beta}; \mathbf{x}, \mathbf{y}) := \Omega(\mathbf{V}(\mathbf{x}; \boldsymbol{\beta})) - \mathbf{y}^\top \mathbf{V}(\mathbf{x}; \boldsymbol{\beta}), \quad (21)$$

where  $\mathbf{V}(\mathbf{x}; \boldsymbol{\beta}) = [\boldsymbol{\beta}^\top \mathbf{x}_1, \dots, \boldsymbol{\beta}^\top \mathbf{x}_K]^\top$  is the vector of systematic utilities, and  $\Omega(\mathbf{V}) = \sup_{\mathbf{p} \in \Delta} \{\mathbf{p}^\top \mathbf{V} - \Lambda(\mathbf{p})\}$  is the surplus function. The term  $\mathbf{y}^\top \mathbf{V}(\mathbf{x}; \boldsymbol{\beta})$  represents the utility of the observed choice via the inner product with the ground-truth one-hot vector  $\mathbf{y} \in \{0, 1\}^K$ .

It is necessary to clarify the theoretical justification for treating the discrete realization  $\mathbf{y}$  within this convex analysis framework. The fundamental *Fenchel-Young inequality* is originally defined over the continuous probability simplex  $\Delta$ : for any potential vector  $\mathbf{V}$  and any probability vector  $\mathbf{p} \in \Delta$ , the inequality  $\Omega(\mathbf{V}) + \Lambda(\mathbf{p}) \geq \mathbf{p}^\top \mathbf{V}$  holds universally. Importantly, the realized choice  $\mathbf{y}$  (a one-hot vector) represents a vertex, and thus an extreme point, of the simplex  $\Delta$ . Since  $\mathbf{y} \in \Delta$ , the inequality remains valid when directly applying the observed choice as the dual variable. The canonical Fenchel-Young loss is therefore rigorously defined as the *duality gap* inherent in this inequality:

$$\mathcal{L}_{\text{gap}}(\boldsymbol{\beta}; \mathbf{x}, \mathbf{y}) := \underbrace{\Omega(\mathbf{V}(\mathbf{x})) + \Lambda(\mathbf{y}) - \mathbf{y}^\top \mathbf{V}(\mathbf{x})}_{\geq 0}.$$

Crucially, the Fenchel-Young loss provides a solid statistical guarantee. By construction, the loss constitutes a *proper scoring rule* generated by the convex function  $\Omega$ . This ensures that minimizing the expected risk inherently drives the model to recover the true conditional probabilities of the data-generating process, rather than merely fitting discrete labels.

**Proposition 2** (Proper Scoring). *Let the realized choice  $\mathbf{y}$  be drawn from a true conditional probability distribution  $\mathbf{p}^* \in \Delta$ , such that  $\mathbb{E}[\mathbf{y}] = \mathbf{p}^*$ . Assume the surplus function  $\Omega$  is strictly convex and differentiable. The expected Fenchel-Young loss, defined as  $\mathcal{R}(\mathbf{V}) = \mathbb{E}_{\mathbf{y} \sim \mathbf{p}^*}[\ell_{\text{FY}}(\mathbf{V}; \mathbf{y})]$ , is minimized if and only if the model's predicted probability distribution  $\hat{\mathbf{p}} = \nabla \Omega(\mathbf{V})$  exactly matches the true distribution  $\mathbf{p}^*$ .*

*Proof.* Recall that the operational Fenchel-Young loss is given by  $\ell_{\text{FY}}(\mathbf{V}; \mathbf{y}) = \Omega(\mathbf{V}) - \mathbf{y}^\top \mathbf{V}$ . We consider the population risk minimization problem:

$$\min_{\mathbf{V}} \mathcal{R}(\mathbf{V}) = \mathbb{E}_{\mathbf{y} \sim \mathbf{p}^*} [\Omega(\mathbf{V}) - \mathbf{y}^\top \mathbf{V}]. \quad (22)$$

By the linearity of expectation, and noting that  $\Omega(\mathbf{V})$  is deterministic with respect to the sampling of  $\mathbf{y}$ , the objective function can be rewritten as:

$$\mathcal{R}(\mathbf{V}) = \Omega(\mathbf{V}) - \mathbb{E}_{\mathbf{y} \sim \mathbf{p}^*} [\mathbf{y}]^\top \mathbf{V}. \quad (23)$$

Since  $\mathbf{y}$  is a one-hot vector representation of the choice, its expectation is precisely the true probability vector, i.e.,  $\mathbb{E}_{\mathbf{y} \sim \mathbf{p}^*} [\mathbf{y}] = \mathbf{p}^*$ . Substituting this back yields:

$$\mathcal{R}(\mathbf{V}) = \Omega(\mathbf{V}) - (\mathbf{p}^*)^\top \mathbf{V}. \quad (24)$$

Since  $\Omega$  is strictly convex, the risk function  $\mathcal{R}(\mathbf{V})$  is also strictly convex with respect to  $\mathbf{V}$  (up to a shift by a linear term). A necessary and sufficient condition for optimality is that the gradient of  $\mathcal{R}(\mathbf{V})$  vanishes:

$$\nabla_{\mathbf{V}} \mathcal{R}(\mathbf{V}) = \nabla \Omega(\mathbf{V}) - \mathbf{p}^* = 0. \quad (25)$$

Rearranging the terms, the optimal condition requires:

$$\nabla\Omega(\mathbf{V}) = \mathbf{p}^*. \quad (26)$$

By the definition of the model’s prediction mapping in PUMs,  $\hat{\mathbf{p}} := \nabla\Omega(\mathbf{V})$ . Therefore, the stationary point satisfies  $\hat{\mathbf{p}} = \mathbf{p}^*$ . Due to the strict convexity of  $\Omega$ , this global minimum is unique in terms of the predicted distribution. Thus, minimizing the FYLoss naturally enforces probability matching.  $\square$

In the context of parameter estimation, the term  $\Lambda(\mathbf{y})$  depends exclusively on the fixed observed label  $\mathbf{y}$  and is independent of the utility parameters  $\beta$ . It therefore acts merely as an additive constant. Consequently, omitting  $\Lambda(\mathbf{y})$  simplifies the operational objective function in Eq. (21) without altering the gradient dynamics or the location of the optimal solution.

The estimation problem over a dataset of  $N$  samples is formulated as the Empirical Risk Minimization (ERM) of the FYLoss:

$$\min_{\beta} \mathcal{J}(\beta) = \frac{1}{N} \sum_{n=1}^N \left( \Omega(\mathbf{V}_n; \beta) - \mathbf{y}_n^\top \mathbf{V}_n \right), \quad (27)$$

where  $\mathbf{V}_n = \mathbf{V}(\mathbf{x}_n; \beta)$  denotes the utility vector for the  $n$ -th sample.

### 3.3 Geometric Interpretation of the Fenchel-Young Estimator

The Fenchel-Young estimation framework admits a profound geometric interpretation that links convex analysis to statistical consistency. Fundamentally, the estimation process operates on the landscape defined by the surplus function  $\Omega$ . A candidate parameter vector  $\beta$  maps attributes  $\mathbf{x}$  to systematic utilities  $\mathbf{V}$ , which in turn induce a predicted probability distribution via the gradient map  $\hat{\mathbf{p}} = \nabla\Omega(\mathbf{V})$ . Rather than forcing a literal geometric projection of empirical labels onto the model manifold, the optimization of  $\beta$  minimizes the Fenchel-Young loss, a divergence measure rigorously defined as the duality gap between the prediction and the realization.

Although evaluating this gap against a discrete vertex  $\mathbf{y}$  (the observed choice) is performed pointwise, minimizing this loss over the population drives the predicted gradients to align with the true conditional probabilities in expectation. Unlike generic loss functions (such as squared error) that may impose an extrinsic geometry mismatched with the choice model, the Fenchel-Young loss is endogenous: it is the unique Bregman divergence generated by the very same potential function  $\Omega$  that governs the probability generation. This intrinsic consistency renders the Fenchel-Young estimator theoretically natural for PUMs, ensuring that the metric used for estimation is structurally congruent with the mechanism used for prediction.

#### 3.3.1 Bregman Divergence

In the discrete choice setting, the observed label is represented as a one-hot vector  $\mathbf{y} = \mathbf{e}_y$ , and the model prediction is the probability vector

$$\mathbf{p} = \nabla_{\mathbf{V}}\Omega(\mathbf{V}) \in \Delta, \quad (28)$$

i.e., the gradient of the surplus function. Thus  $\ell_{\text{FY}}$  is nonnegative, and it vanishes exactly when the predicted distribution  $\mathbf{p}$  matches the target distribution  $\mathbf{y}$  (so that  $\mathbf{y} \in \partial\Omega(\mathbf{V})$ ).

Using convex conjugacy, the Fenchel–Young loss can be written as a Bregman divergence in probability space. Recall that, by definition of the conjugate,

$$\Omega(\mathbf{V}) = \sup_{\mathbf{p} \in \Delta} \left\{ \mathbf{p}^\top \mathbf{V} - \Lambda(\mathbf{p}) \right\}, \quad \mathbf{p} = \nabla \Omega(\mathbf{V}) \iff \mathbf{V} = \nabla \Lambda(\mathbf{p}). \quad (29)$$

Evaluating the supremum at  $\mathbf{p}$  gives

$$\Omega(\mathbf{V}) = \mathbf{p}^\top \mathbf{V} - \Lambda(\mathbf{p}). \quad (30)$$

Substituting this into the Fenchel–Young loss yields

$$\ell_{\text{FY}}(\mathbf{V}; \mathbf{y}) = (\mathbf{p}^\top \mathbf{V} - \Lambda(\mathbf{p})) + \Lambda(\mathbf{y}) - \mathbf{y}^\top \mathbf{V} \quad (31)$$

$$= \Lambda(\mathbf{y}) - \Lambda(\mathbf{p}) - (\mathbf{y} - \mathbf{p})^\top \mathbf{V} \quad (32)$$

$$= \Lambda(\mathbf{y}) - \Lambda(\mathbf{p}) - (\mathbf{y} - \mathbf{p})^\top \nabla \Lambda(\mathbf{p}), \quad (33)$$

where in the last step we used  $\mathbf{V} = \nabla \Lambda(\mathbf{p})$ . The right-hand side is exactly the Bregman divergence generated by  $\Lambda$ :

$$\mathbb{D}_\Lambda(\mathbf{y} \parallel \mathbf{p}) := \Lambda(\mathbf{y}) - \Lambda(\mathbf{p}) - (\mathbf{y} - \mathbf{p})^\top \nabla \Lambda(\mathbf{p}). \quad (34)$$

Therefore,

$$\ell_{\text{FY}}(\mathbf{V}; \mathbf{y}) = \mathbb{D}_\Lambda(\mathbf{y} \parallel \mathbf{p}) \quad (35)$$

so the Fenchel–Young loss is the Bregman divergence between the target distribution  $\mathbf{y}$  and the predicted distribution  $\mathbf{p}$ , with generator  $\Lambda$ .

### 3.3.2 Geometric Picture

The Bregman divergence  $\mathbb{D}_\Lambda(\mathbf{y} \parallel \mathbf{p})$  has a simple geometric meaning: it measures how much  $\Lambda(\mathbf{y})$  exceeds the first-order (affine) approximation of  $\Lambda$  around  $\mathbf{p}$ . In other words, it is the vertical gap between the value of  $\Lambda$  at  $\mathbf{y}$  and the tangent hyperplane of  $\Lambda$  at  $\mathbf{p}$ . This gap is always nonnegative by convexity, and it is zero if and only if  $\mathbf{y} = \mathbf{p}$ .

From this viewpoint, minimizing the Fenchel–Young loss over the dataset is equivalent to projecting the empirical distribution (the aggregate of observed one-hot labels) onto the manifold of model distributions

$$\mathcal{M} = \left\{ \mathbf{p}(\cdot; \boldsymbol{\beta}) = \nabla \Omega(\mathbf{V}(\cdot; \boldsymbol{\beta})) : \boldsymbol{\beta} \in \mathbb{R}^d \right\}$$

under the Bregman geometry induced by  $\Lambda$ . Specifically, the estimator  $\hat{\boldsymbol{\beta}}$  seeks the distribution on  $\mathcal{M}$  that is closest to the data-generating process in terms of the expected divergence. Rather than matching each realization pointwise, this process constitutes an *information projection* of the observed statistics onto the model family, aligning the predicted probabilities with the realized choices in expectation.

### 3.3.3 Equivalence to Maximum Likelihood Estimation for Multinomial Logit

For the Shannon-entropy regularizer  $\Lambda_{\text{Shannon}}(\mathbf{p}) = \mu \sum_i p_i \log p_i$  with a smoothing parameter  $\mu > 0$ , the convex conjugate is the scaled log-sum-exp potential  $\Omega_\mu(\mathbf{V}) = \mu \log \sum_i \exp(V_i/\mu)$ , and the induced PUM coincides with the MNL model with temperature  $\mu$ . In this case, the Fenchel–Young loss reduces exactly to the negative log-likelihood scaled by  $\mu$ .

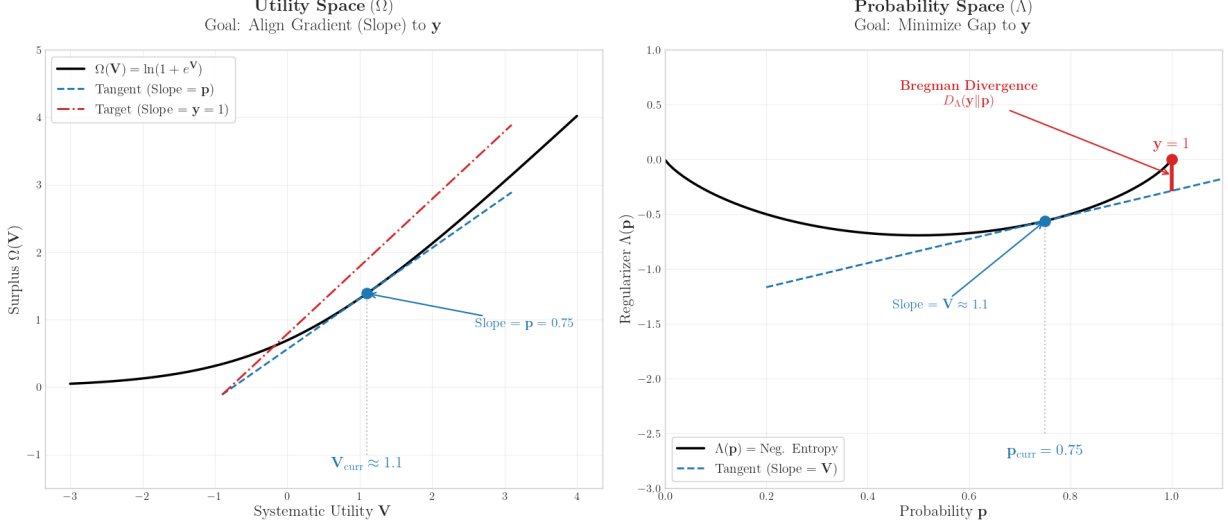


Figure 1: **Geometric Interpretation of Fenchel-Young Estimation: Duality between Utility and Probability Spaces.** The Left Panel displays the surplus function  $\Omega(\mathbf{V})$  in the utility space. The model prediction  $\mathbf{p}$  corresponds to the gradient (slope) of the tangent at the current utility  $\mathbf{V}_{\text{curr}}$ . The estimation goal is to align this slope with the target slope defined by the observed label  $\mathbf{y}$ . The Right Panel displays the conjugate regularization function  $\Lambda(\mathbf{p})$  in the probability space. Here, the Fenchel-Young loss is visualized as the Bregman divergence  $D_{\Lambda}(\mathbf{y}||\mathbf{p})$ , i.e., the vertical gap between the function value  $\Lambda(\mathbf{y})$  and the tangent hyperplane constructed at the prediction  $\mathbf{p}$ . Crucially, the two views are mathematically equivalent via the Legendre-Fenchel transform: the slope in the left panel ( $\mathbf{p}$ ) becomes the coordinate in the right panel, and the slope in the right panel ( $\mathbf{V}$ ) corresponds to the coordinate in the left.

**Proposition 3** (FY vs. MLE for Multinomial Logit). *Consider the MNL model with utilities  $V_{ni}(\boldsymbol{\beta}) = \boldsymbol{\beta}^{\top} \mathbf{x}_{ni}$  and temperature  $\mu$ , where the choice probabilities are given by*

$$p_{ni}(\boldsymbol{\beta}) = \frac{\exp(V_{ni}(\boldsymbol{\beta})/\mu)}{\sum_j \exp(V_{nj}(\boldsymbol{\beta})/\mu)}.$$

For an observation  $(\mathbf{x}_n, y_n)$ , the associated Fenchel-Young loss with scaled Shannon entropy is

$$\ell_{\text{FY}}(\boldsymbol{\beta}; \mathbf{x}_n, y_n) = \mu \log \sum_j \exp(\boldsymbol{\beta}^{\top} \mathbf{x}_{nj}/\mu) - \boldsymbol{\beta}^{\top} \mathbf{x}_{ny_n}.$$

This coincides with  $\mu$  times the negative log-likelihood:  $\ell_{\text{FY}} = \mu \cdot (-\log p_{ny_n}(\boldsymbol{\beta}))$ . Since  $\mu$  is a strictly positive constant, the FY estimator and the maximum likelihood estimator for this model are identical:

$$\hat{\boldsymbol{\beta}}_{\text{FY}} = \hat{\boldsymbol{\beta}}_{\text{MLE}}.$$

Intuitively, this equivalence follows from the fact that the Bregman divergence induced by the scaled negative Shannon entropy is exactly the scaled Kullback-Leibler divergence. For one-hot labels  $\mathbf{e}_{y_n}$  and model probabilities  $\mathbf{p}_n(\boldsymbol{\beta})$ , the Fenchel-Young loss can be written as

$$\ell_{\text{FY}}(\boldsymbol{\beta}; \mathbf{x}_n, y_n) = \mu \mathbb{D}_{\text{KL}}(\mathbf{e}_{y_n} || \mathbf{p}_n(\boldsymbol{\beta})),$$

up to an additive constant independent of  $\beta$ . Minimizing the average FY loss therefore amounts to minimizing the empirical KL divergence between empirical label distributions and model predictions, which is exactly maximum likelihood estimation for the multinomial logit model.

### 3.4 Convexity Analysis

A major advantage of the Fenchel-Young estimation framework is that the convexity of the optimization problem follows directly from the definition of PUMs, without requiring complex analysis of the Hessian or log-concavity conditions.

**Proposition 4** (Global Convexity of PUM Estimation). *For any PUM defined by a convex regularizer  $\Lambda$ , the estimation problem (27) is a convex optimization problem.*

*Proof.* The objective function is a sum of terms  $\ell_{\text{FY}}(\beta; \mathbf{x}, y)$ . Recall that  $\Omega(\mathbf{V})$  is defined as the convex conjugate (Fenchel-Legendre transform) of the regularizer  $\Lambda(\mathbf{p})$ . A fundamental result in convex analysis states that the conjugate of any function is always a convex function.

Since the systematic utility  $\mathbf{V}(\mathbf{x})$  is a linear function of the parameters  $\beta$ , and convexity is preserved under affine composition, the term  $\Omega(\mathbf{V}(\beta))$  is convex with respect to  $\beta$ . The second term,  $-\beta^\top \mathbf{x}_{n,y_n}$ , is linear in  $\beta$ .

Therefore, the loss function  $\ell_{\text{FY}}$ , being the sum of a convex function and a linear function, is globally convex with respect to  $\beta$ . This guarantees that any local minimum of (27) is a global minimum, ensuring the feasibility of numerical optimization.  $\square$

### 3.5 Solution Approach

Having established the global convexity of the Fenchel-Young estimation problem in Proposition 4, the optimization landscape is guaranteed to be free of local minima. Consequently, the estimation task simplifies to a standard convex optimization problem, where the global optimum can be reliably recovered via iterative first-order methods, provided that the gradient of the objective function is computable. A remarkable property of the proposed framework is that, for any admissible PUM, regardless of the specific complexity of the choice kernel, the gradient with respect to the utility parameters  $\beta$  always simplifies to a unified and physically interpretable form:

$$\nabla_{\beta} \mathcal{J}(\beta) = \frac{1}{N} \sum_{n=1}^N \left( \underbrace{\sum_{i \in \mathcal{C}} p_{ni}(\beta) \mathbf{x}_{ni}}_{\text{Predicted Expected Features}} - \underbrace{\mathbf{x}_{n,y_n}}_{\text{Observed Features}} \right). \quad (36)$$

This formulation reveals that the optimization process is fundamentally driven by moment matching: the solver iteratively adjusts  $\beta$  to align the model’s predicted aggregate attributes with the empirical observations, with the specific of the PUM entering solely through the calculation of the probability weights  $p_{ni}(\beta)$ .

Crucially, while the gradient structure remains unified, the computational complexity of evaluating the probability weights  $p_{ni}(\beta)$  varies significantly across specifications. Unlike MNL, which admits a closed-form expression, determining the choice probabilities for a general perturbation function  $\Lambda$  necessitates solving the primal convex optimization problem inherent to the PUM definition. This implies that the gradient evaluation involves an embedded optimization layer: for every observation  $n$  at every iterative step, the solver must numerically retrieve the optimal vector  $\mathbf{p}_n$ . Although this nested structure does not compromise the global convergence properties of the

outer algorithm, it inevitably increases the computational cost per iteration, potentially creating a bottleneck for large-scale applications.

Fortunately, within the Fenchel–Young framework, we can circumvent this computational bottleneck by exploiting the variational definition of the conjugate function  $\Omega$ . Instead of treating the probability evaluation as a subroutine to be solved to optimality at every step, we can substitute the definition of  $\Omega(\mathbf{V}_n)$  back into the empirical risk objective. This allows us to reformulate the original nested minimization problem into a single, unified *convex-concave saddle point problem*. By lifting the probability vectors from implicit mappings to explicit optimization variables, we arrive at the following minimax formulation:

$$\min_{\boldsymbol{\beta} \in \mathbb{R}^d} \max_{\mathbf{p}^\circ \in \Delta^N} \mathcal{L}(\boldsymbol{\beta}, \mathbf{p}^\circ) := \frac{1}{N} \sum_{n=1}^N \left[ (\mathbf{p}_n - \mathbf{y}_n)^\top \mathbf{V}_n(\boldsymbol{\beta}) - \Lambda(\mathbf{p}_n) \right], \quad (37)$$

where  $\mathbf{p}^\circ = (\mathbf{p}_1, \dots, \mathbf{p}_N)$  denotes the stacked vector of choice probabilities for all observations, and  $\Delta^N = \Delta \times \dots \times \Delta$  is the Cartesian product of simplexes.

It can be verified that this objective is globally convex (specifically, linear) with respect to  $\boldsymbol{\beta}$  and globally concave with respect to the collection of probability vectors  $\mathbf{p}^\circ$ . To address these challenges while strictly avoiding expensive inner-loop optimization, we employ the *projected extragradient method* (Mokhtari et al., 2020). This algorithm utilizes a prediction-correction mechanism to stabilize the update trajectory and guarantees global convergence for smooth operators.

Let  $\tau > 0$  and  $\sigma > 0$  denote the primal and dual step sizes, respectively. At iteration  $k$ , we first compute a temporary look-ahead point  $(\tilde{\boldsymbol{\beta}}^{(k)}, \tilde{\mathbf{p}}^{\circ(k)})$  by taking a standard gradient step from the current position:

$$\tilde{\mathbf{p}}_n^{(k)} = \mathcal{P}_\Delta \left( \mathbf{p}_n^{(k)} + \sigma \left[ \mathbf{V}_n(\boldsymbol{\beta}^{(k)}) - \nabla \Lambda(\mathbf{p}_n^{(k)}) \right] \right), \quad \forall n = 1, \dots, N, \quad (38a)$$

$$\tilde{\boldsymbol{\beta}}^{(k)} = \boldsymbol{\beta}^{(k)} - \tau \left[ \frac{1}{N} \sum_{n=1}^N \mathbf{X}_n^\top (\mathbf{p}_n^{(k)} - \mathbf{y}_n) \right], \quad (38b)$$

where  $\mathcal{P}_\Delta(\cdot)$  denotes the Euclidean projection onto the probability simplex, and  $\nabla \Lambda(\cdot)$  is the gradient of the perturbation function. Note that the bracket term in the second equation corresponds precisely to the gradient of the primal objective  $\nabla J(\boldsymbol{\beta})$ , i.e., Eq.(36), but here the probability vector  $\mathbf{p}_n$  is treated as an independent dual variable rather than an implicit function of  $\boldsymbol{\beta}$ .

We then update the variables using the gradients evaluated at the predicted point, rather than the current point, to damp oscillations:

$$\mathbf{p}_n^{(k+1)} = \mathcal{P}_\Delta \left( \mathbf{p}_n^{(k)} + \sigma \left[ \mathbf{V}_n(\tilde{\boldsymbol{\beta}}^{(k)}) - \nabla \Lambda(\tilde{\mathbf{p}}_n^{(k)}) \right] \right), \quad \forall n = 1, \dots, N, \quad (39a)$$

$$\boldsymbol{\beta}^{(k+1)} = \boldsymbol{\beta}^{(k)} - \tau \left[ \frac{1}{N} \sum_{n=1}^N \mathbf{X}_n^\top (\tilde{\mathbf{p}}_n^{(k)} - \mathbf{y}_n) \right]. \quad (39b)$$

According to Mokhtari et al. (2020), the above projected extragradient method can achieve a convergence rate of  $\mathcal{O}(1/k)$ , which is sublinear. However, for the significant subclass of additive separable PUMs (including Sparsemax, Cauchy, among others), we can exploit the structural decomposability of the regularizer to achieve substantially faster convergence. In these cases, the perturbation function separates as  $\Lambda(\mathbf{p}) = \sum_{i \in \mathcal{C}} h(p_i)$ , where  $h$  is a strictly convex scalar function. This structure decouples the primal optimization problem, allowing the optimal choice probabilities  $\mathbf{p}_n(\boldsymbol{\beta})$  to be recovered through a computationally efficient, semi-analytical mapping rather than

a high-dimensional iterative solver. Specifically, the probability for alternative  $i$  is given by the inverse of the derivative of the regularizer:

$$p_{ni}(\boldsymbol{\beta}) = \psi(V_{ni}(\boldsymbol{\beta}) - \lambda_n), \quad \text{with } \psi = (h')^{-1}, \quad (40)$$

where  $\lambda_n \in \mathbb{R}$  is the unique Lagrange multiplier (normalization constant) determined by solving the scalar root-finding equation:

$$\sum_{j \in \mathcal{C}} \psi(V_{nj}(\boldsymbol{\beta}) - \lambda_n) = 1. \quad (41)$$

The numerical resolution of this equation is both well-posed and highly efficient. Since the mapping  $\psi(\cdot)$  is strictly increasing (being the inverse derivative of a strictly convex function), the aggregate function  $G(\lambda_n) = \sum_{j \in \mathcal{C}} \psi(V_{nj} - \lambda_n) - 1$  is strictly monotonically decreasing with respect to  $\lambda_n$ . This monotonicity guarantees the existence and uniqueness of the Lagrange multiplier, enabling the use of standard root-finding algorithms with guaranteed convergence. For instance, derivative-free methods such as the golden section search offer robust global convergence with a linear rate. More aggressively, if  $\psi$  is differentiable, Newton’s method can be employed to achieve a quadratic convergence rate, effectively doubling the digits of precision at every step and typically resolving  $\lambda_n$  to machine tolerance within a few iterations.

Consequently, since the inner forward problem is reduced to a low-cost scalar operation, the computational bottleneck associated with the nested optimization is effectively eliminated. By combining this rapid evaluation of choice probabilities with the analytical gradient derived in Eq.(36), we can solve the Fenchel–Young estimation problem using advanced gradient-based optimization algorithms that exploit the objective’s smoothness and convexity. A quintessential example is Nesterov’s Accelerated Gradient (NAG; Nesterov, 1983). Unlike standard gradient descent, NAG incorporates a momentum term to correct the search trajectory based on previous iterations. This modification allows the algorithm to achieve the theoretically optimal convergence rate of  $\mathcal{O}(1/k^2)$  for smooth convex functions, ensuring that the global optimum is reached with significantly fewer gradient evaluations.

### 3.6 Asymptotic Properties

In addition to convexity and numerical tractability, a viable estimation method must also possess sound large-sample statistical behavior. In this section, we study the asymptotic properties of Fenchel–Young estimators for general PUMs. Our goal is twofold. First, we show that under mild regularity conditions and correct model specification, the FY estimator consistently recovers the true parameter vector as the sample size grows, i.e., it converges in probability to the data-generating parameter. Second, we establish an asymptotic normality result: after appropriate rescaling by  $\sqrt{N}$ , the estimation error converges in distribution to a multivariate normal law with a well-defined covariance matrix.

We proceed by presenting two lemmas first.

**Lemma 1** (Continuity and domination of the FY loss). *Let  $\ell_{\text{FY}}(\boldsymbol{\beta}; \mathbf{x}, \mathbf{y})$  denote the Fenchel–Young loss associated with a PUM, and let  $\mathcal{B} \subset \mathbb{R}^d$  be a compact parameter set. Assume that the data are generated under a probability measure  $\mathbb{P}^*$  on  $\mathcal{X} \times \mathcal{Y}$ , where  $\mathcal{Y} = \{\mathbf{e}_1, \dots, \mathbf{e}_K\}$ . Then the following continuity and domination conditions hold:*

1. For each  $(\mathbf{x}, \mathbf{y})$ , the map

$$\boldsymbol{\beta} \mapsto \ell_{\text{FY}}(\boldsymbol{\beta}; \mathbf{x}, \mathbf{y})$$

is continuous on  $\mathcal{B}$ .

2. There exists an integrable function  $M : \mathcal{X} \times \mathcal{Y} \rightarrow [0, \infty)$  such that

$$|\ell_{\text{FY}}(\boldsymbol{\beta}; \mathbf{x}, \mathbf{y})| \leq M(\mathbf{x}, \mathbf{y})$$

for all  $\boldsymbol{\beta} \in \mathcal{B}$  and for  $\mathbb{P}^*$ -almost all  $(\mathbf{x}, \mathbf{y})$ .

*Proof.* See Appendix A. □

**Lemma 2** (Identifiability of the PUM parameter). *Fix the dispersion parameter  $\mu$ . Let  $\mathbf{x} \mapsto \mathbf{V}(\mathbf{x}; \boldsymbol{\beta})$  denote the systematic utilities and  $\mathbf{p}(\mathbf{x}; \boldsymbol{\beta}) = \nabla_{\mathbf{V}} \Omega(\mathbf{V}(\mathbf{x}; \boldsymbol{\beta}))$  the corresponding choice probabilities of a PUM. Assume the standard rank condition so that  $\mathbf{V}(\mathbf{x}; \boldsymbol{\beta}_1) = \mathbf{V}(\mathbf{x}; \boldsymbol{\beta}_2)$  for almost all  $\mathbf{x}$  implies  $\boldsymbol{\beta}_1 = \boldsymbol{\beta}_2$ . Then  $\boldsymbol{\beta}$  is identifiable in the sense that*

$$\mathbf{p}(\mathbf{x}; \boldsymbol{\beta}_1) = \mathbf{p}(\mathbf{x}; \boldsymbol{\beta}_2) \quad \text{for almost all } \mathbf{x} \implies \boldsymbol{\beta}_1 = \boldsymbol{\beta}_2.$$

*Proof.* If  $\mathbf{p}(\mathbf{x}; \boldsymbol{\beta}_1) = \mathbf{p}(\mathbf{x}; \boldsymbol{\beta}_2)$  for almost all  $\mathbf{x}$ , then, by the PUM duality  $\mathbf{p} = \nabla_{\mathbf{V}} \Omega(\mathbf{V})$  and the injectivity of  $\nabla \Omega$ , we have  $\mathbf{V}(\mathbf{x}; \boldsymbol{\beta}_1) = \mathbf{V}(\mathbf{x}; \boldsymbol{\beta}_2)$  for almost all  $\mathbf{x}$ . The rank condition on the regressors then implies  $\boldsymbol{\beta}_1 = \boldsymbol{\beta}_2$ , which proves the claim. □

Next, we present the consistency theorem for the FY estimators for PUMs.

**Theorem 1** (Consistency of FY Estimator for PUM). *Let  $\{(\mathbf{X}_n, \mathbf{Y}_n)\}_{n=1}^N$  be i.i.d. random vectors from  $\mathbb{P}^*$  and consider a PUM with FY loss  $\ell_{\text{FY}}(\boldsymbol{\beta}; \mathbf{x}, \mathbf{y})$ . Assume the model is well-specified, i.e., there exists a unique  $\boldsymbol{\beta}^* \in \mathcal{B}$  such that*

$$\mathbb{E}_{\mathbb{P}^*}[\mathbf{Y} \mid \mathbf{X} = \mathbf{x}] = \mathbf{p}(\mathbf{x}; \boldsymbol{\beta}^*) \quad \text{almost surely,}$$

and that the continuity and identifiability conditions in Lemmas 1 and 2 hold.

Let

$$\hat{\boldsymbol{\beta}}_N \in \arg \min_{\boldsymbol{\beta} \in \mathcal{B}} \frac{1}{N} \sum_{n=1}^N \ell_{\text{FY}}(\boldsymbol{\beta}; \mathbf{X}_n, \mathbf{Y}_n)$$

be any empirical FY minimizer. Then the population FY risk  $R(\boldsymbol{\beta}) := \mathbb{E}_{\mathbb{P}^*}[\ell_{\text{FY}}(\boldsymbol{\beta}; \mathbf{X}, \mathbf{Y})]$  is uniquely minimized at  $\boldsymbol{\beta}^*$ , and

$$\hat{\boldsymbol{\beta}}_N \xrightarrow{p} \boldsymbol{\beta}^* \quad \text{as } N \rightarrow \infty.$$

*Proof.* See Appendix A. □

Next, under slightly stronger regularity conditions, we analyze the convergence rate of the FY estimators.

**Theorem 2** (Asymptotic Normality of the FY Estimator). *Let  $\hat{\boldsymbol{\beta}}_N$  be the estimator obtained by minimizing the empirical Fenchel–Young loss over a dataset of  $N$  i.i.d. samples generated from a well-specified PUM with true parameter  $\boldsymbol{\beta}^*$ . Assume the following regularity conditions hold:*

1. **Regularity of  $\Omega$ :** *The surplus function  $\Omega$  is twice continuously differentiable in a neighborhood of  $\mathbf{V}(\mathbf{X}; \boldsymbol{\beta}^*)$  almost surely.*
2. **Non-singularity:** *The expected Hessian matrix  $\mathbf{H}(\boldsymbol{\beta}^*) := \mathbb{E}[\nabla^2 \ell_{\text{FY}}(\boldsymbol{\beta}^*; \mathbf{X}, \mathbf{Y})]$  is positive definite.*
3. **Finite Moments:**  *$\mathbb{E}[\|\mathbf{X}\|^2] < \infty$  and the covariance of the gradient  $\mathbf{J}(\boldsymbol{\beta}^*)$  is finite.*

Then, as  $N \rightarrow \infty$ ,

$$\sqrt{N}(\hat{\boldsymbol{\beta}}_N - \boldsymbol{\beta}^*) \xrightarrow{d} \mathcal{N}(\mathbf{0}, \mathbf{V}_{\text{sand}}),$$

where the asymptotic variance is given by the sandwich form:

$$\mathbf{V}_{\text{sand}} = \mathbf{H}(\boldsymbol{\beta}^*)^{-1} \mathbf{J}(\boldsymbol{\beta}^*) \mathbf{H}(\boldsymbol{\beta}^*)^{-1}. \quad (42)$$

*Proof.* Let  $\ell_n(\boldsymbol{\beta}) := \ell_{\text{FY}}(\boldsymbol{\beta}; \mathbf{X}_n, \mathbf{Y}_n)$  denote the loss for the  $n$ -th observation, and let  $\mathbf{g}_n(\boldsymbol{\beta}) := \nabla \ell_n(\boldsymbol{\beta})$  denote its gradient. The estimator satisfies the empirical first-order condition  $\frac{1}{N} \sum_{n=1}^N \mathbf{g}_n(\hat{\boldsymbol{\beta}}_N) = \mathbf{0}$ . With Proposition 2, we have confirmed the Fisher consistency, implying  $\mathbb{E}[\mathbf{g}(\boldsymbol{\beta}^*)] = \mathbf{0}$ .

Since  $\hat{\boldsymbol{\beta}}_N \xrightarrow{p} \boldsymbol{\beta}^*$  (Theorem 1), we expand the empirical gradient around  $\boldsymbol{\beta}^*$ :

$$\mathbf{0} = \frac{1}{N} \sum_{n=1}^N \mathbf{g}_n(\hat{\boldsymbol{\beta}}_N) = \frac{1}{N} \sum_{n=1}^N \mathbf{g}_n(\boldsymbol{\beta}^*) + \left( \frac{1}{N} \sum_{n=1}^N \nabla^2 \ell_n(\tilde{\boldsymbol{\beta}}_N) \right) (\hat{\boldsymbol{\beta}}_N - \boldsymbol{\beta}^*),$$

where  $\tilde{\boldsymbol{\beta}}_N$  lies on the line segment between  $\hat{\boldsymbol{\beta}}_N$  and  $\boldsymbol{\beta}^*$ . Rearranging terms and scaling by  $\sqrt{N}$ :

$$\sqrt{N}(\hat{\boldsymbol{\beta}}_N - \boldsymbol{\beta}^*) = - \left( \frac{1}{N} \sum_{n=1}^N \nabla^2 \ell_n(\tilde{\boldsymbol{\beta}}_N) \right)^{-1} \left( \frac{1}{\sqrt{N}} \sum_{n=1}^N \mathbf{g}_n(\boldsymbol{\beta}^*) \right).$$

We analyze the convergence of the two components:

- **Hessian Convergence:** By the Uniform Law of Large Numbers and the assumed regularity of the Hessian, the bracketed term converges in probability to the population Hessian:

$$\frac{1}{N} \sum_{n=1}^N \nabla^2 \ell_n(\tilde{\boldsymbol{\beta}}_N) \xrightarrow{p} \mathbb{E}[\nabla^2 \ell(\boldsymbol{\beta}^*)] = \mathbf{H}(\boldsymbol{\beta}^*).$$

Note that for PUMs, the Hessian takes the form  $\nabla^2 \ell(\boldsymbol{\beta}) = \mathbf{X}[\nabla^2 \Omega(\mathbf{V})] \mathbf{X}^\top$ .

- **Central Limit Theorem:** The term  $\frac{1}{\sqrt{N}} \sum \mathbf{g}_n(\boldsymbol{\beta}^*)$  is a sum of i.i.d. zero-mean random vectors with covariance matrix:

$$\mathbf{J}(\boldsymbol{\beta}^*) := \mathbb{E}[\mathbf{g}(\boldsymbol{\beta}^*) \mathbf{g}(\boldsymbol{\beta}^*)^\top].$$

By the Multivariate CLT, this term converges in distribution to  $\mathcal{N}(\mathbf{0}, \mathbf{J}(\boldsymbol{\beta}^*))$ .

Combining these results via Slutsky's Theorem, we obtain:

$$\sqrt{N}(\hat{\boldsymbol{\beta}}_N - \boldsymbol{\beta}^*) \xrightarrow{d} -\mathbf{H}^{-1} \cdot \mathcal{N}(\mathbf{0}, \mathbf{J}) \sim \mathcal{N}(\mathbf{0}, \mathbf{H}^{-1} \mathbf{J} \mathbf{H}^{-1}).$$

□

It is crucial to distinguish between two cases regarding the asymptotic efficiency:

- **Multinomial Logit:** For MNL, the Fenchel–Young loss coincides with the negative log-likelihood. By the Bartlett identities, the expected Hessian equals the covariance of the score ( $\mathbf{H} = \mathbf{J} = \mathcal{I}_{\text{Fisher}}^{-1}$ ). The sandwich variance simplifies to  $\mathcal{I}_{\text{Fisher}}^{-1}$ , achieving the Cramér-Rao lower bound (asymptotic efficiency).

- **Sparsemax:** For PUMs with sparse choice kernels, while consistency holds, the regularity conditions required for standard asymptotic normality (specifically twice continuous differentiability) may not hold everywhere due to the non-smoothness of the Sparsemax transform at the boundaries of the support. In these cases,  $\mathbf{H} \neq \mathbf{J}$  generally. The matrix  $\mathbf{H}$  reflects the curvature of the convex conjugate  $\Omega$ , which may have flat regions (zero curvature) where probabilities are sparse, whereas  $\mathbf{J}$  reflects the variance of the residuals. Consequently,  $\mathbf{V}_{\text{sand}} \succeq \mathcal{I}_{\text{Fisher}}^{-1}$  (in the Löwner order), implying that the Fenchel–Young estimator, while robust, may be theoretically less efficient than the MLE in the large-sample limit.

## 4 Wasserstein Distance-based Distributionally Robust Estimation

### 4.1 The Curse of Limited Data

Standard Empirical Risk Minimization or ERM strategies, including the proposed Fenchel-Young framework, operate under the tacit assumption that the empirical distribution  $\hat{\mathbb{P}}_N$ , constructed from observed samples, serves as a sufficient statistic for the true underlying data-generating distribution  $\mathbb{P}$ . Asymptotically, as the sample size  $N \rightarrow \infty$ , we know that  $\hat{\mathbb{P}}_N$  converges to  $\mathbb{P}$ , guaranteeing the consistency of the estimator. However, in the regime of limited data, this asymptotic promise breaks down. The empirical distribution becomes a sparse, high-variance approximation that fails to capture the true support and tail behavior of the underlying preference distribution. Consequently, any estimator that strictly minimizes risk with respect to  $\hat{\mathbb{P}}_N$  tends to overfit the idiosyncratic noise of the finite sample rather than capturing the generalized structural parameters.

Crucially, this statistical vulnerability is inherent to the estimation of PUMs due to the fundamental nonlinearity of the choice mechanism. The optimality condition for the Fenchel-Young estimator requires finding the root of the gradient equations:  $\sum_n (\nabla \Omega(\mathbf{V}_n(\boldsymbol{\beta})) - \mathbf{y}_n) \otimes \mathbf{x}_n = \mathbf{0}$ . Here, the mapping from parameters to probabilities,  $\boldsymbol{\beta} \mapsto \nabla \Omega(\mathbf{V}(\boldsymbol{\beta}))$ , involves the choice kernel  $\psi(\cdot)$  (e.g., the projection operator in Sparsemax), which is highly nonlinear. While these estimating equations are consistent, the operation of retrieving parameters from noisy finite data is subject to Jensen’s inequality due to the curvature of the surplus function  $\Omega$ . This induces a systematic finite-sample bias, typically manifesting as magnitude inflation ( $\mathbb{E}[\|\hat{\boldsymbol{\beta}}\|] > \|\boldsymbol{\beta}_{\text{true}}\|$ ), a phenomenon that stems from the geometry of the PUM itself.

Although the Fenchel-Young loss provides numerical stability through bounded gradients, stability does not equate to statistical robustness against sampling error. In small-sample regimes, the discrepancy between the empirical distribution  $\hat{\mathbb{P}}_N$  and the true distribution  $\mathbb{P}$  remains a dominant source of error. To ensure reliable inference under data scarcity, we must therefore go beyond standard ERM. Instead of optimizing solely over the unreliable empirical distribution, we propose a robust modification that explicitly accounts for the distributional uncertainty surrounding  $\hat{\mathbb{P}}_N$ .

### 4.2 Wasserstein Distance-based Formulation and its Convex Dual Formulation

Let  $\mathcal{Z} = \mathcal{X} \times \mathcal{Y} \subseteq \mathbb{R}^d \times \{\mathbf{e}_1, \dots, \mathbf{e}_K\}$  denote the sample space, where  $\mathcal{Y}$  consists of the standard basis vectors in  $\mathbb{R}^K$  representing the  $K$  discrete alternatives. We define the ambiguity set  $\mathcal{B}_\epsilon(\hat{\mathbb{P}}_N)$  as the set of all probability distributions  $\mathbb{Q}$  supported on  $\mathcal{Z}$  such that their Wasserstein distance to the empirical distribution satisfies  $W_c(\mathbb{Q}, \hat{\mathbb{P}}_N) \leq \epsilon$ . The radius  $\epsilon > 0$  serves as a budget for distributional uncertainty.

The choice of the ground metric  $c(z, z')$  is pivotal for the performance of PUM estimation. To capture the distinct nature of continuous attributes and discrete categorical labels, we propose a

hybrid transport cost function. For two data points  $z = (\mathbf{x}, \mathbf{y})$  and  $z' = (\mathbf{x}', \mathbf{y}')$ , we define:

$$c(z, z') \triangleq \|\mathbf{x} - \mathbf{x}'\|_{\mathbf{S}} + \kappa \cdot \mathbb{I}(\mathbf{y} \neq \mathbf{y}'), \quad (43)$$

where  $\|\mathbf{u}\|_{\mathbf{S}} = \sqrt{\mathbf{u}^\top \mathbf{S}^{-1} \mathbf{u}}$  represents the Mahalanobis distance weighted by the empirical covariance matrix  $\mathbf{S}$  of the attributes, and  $\kappa > 0$  is a penalty parameter for label mismatch. This metric induces an anisotropic robustness in the feature space while allowing for controlled label noise to prevent perfect separation.

The primal robust estimation problem is formulated as:

$$\min_{\boldsymbol{\beta}} \sup_{\mathbb{Q} \in \mathcal{B}_\epsilon(\hat{\mathbb{P}}_N)} \mathbb{E}_{\mathbb{Q}} [\ell_{\text{FY}}(\boldsymbol{\beta}; \mathbf{x}, \mathbf{y})], \quad (44)$$

where  $\ell_{\text{FY}}(\boldsymbol{\beta}; \mathbf{x}, \mathbf{y}) = \Omega(\mathbf{V}(\mathbf{x})) - \mathbf{y}^\top \mathbf{V}(\mathbf{x})$  denotes the Fenchel–Young loss derived from the PUM’s surplus function  $\Omega$ , and  $\mathbf{y} \in \mathcal{Y}$  represents the observed choice as a one-hot vector.

#### 4.2.1 Exact Dual Reformulation

We now derive the exact reformulation of the infinite-dimensional distributionally robust problem (44). The primal problem seeks to minimize the worst-case expected loss over the Wasserstein ball  $\mathbb{B}_\epsilon(\hat{\mathbb{P}}_N)$ . Since the Fenchel–Young loss  $\ell_{\text{FY}}(\boldsymbol{\beta}; \mathbf{x}, \mathbf{y})$  is continuous in  $\mathbf{x}$  and the uncertainty set  $\Xi = \mathcal{X} \times \mathcal{Y}$  is a closed subset in Polish space, the strong duality result for Wasserstein DRO holds (Mohajerin Esfahani and Kuhn, 2018). This allows us to rephrase the problem as a minimization over the dual variable  $\gamma \geq 0$  (the Lagrange multiplier for the Wasserstein constraint) and auxiliary variables  $\{s_n\}_{n=1}^N$  representing the worst-case loss for each sample.

**Theorem 3** (Exact Reformulation). *Consider the Fenchel–Young distributionally robust estimator with the hybrid transport cost defined by  $c((\mathbf{x}, \mathbf{y}), (\mathbf{x}', \mathbf{y}')) = \|\mathbf{x} - \mathbf{x}'\|_{\mathbf{S}} + \kappa \mathbb{I}(\mathbf{y} \neq \mathbf{y}')$ . The infinite-dimensional primal problem:*

$$\min_{\boldsymbol{\beta}} \sup_{\mathbb{Q} \in \mathcal{B}_\epsilon(\hat{\mathbb{P}}_N)} \mathbb{E}_{\mathbb{Q}} [\ell_{\text{FY}}(\boldsymbol{\beta}; \mathbf{x}, \mathbf{y})] \quad (45)$$

*is equivalent to the following finite-dimensional convex optimization problem:*

$$\begin{aligned} \min_{\boldsymbol{\beta}, \gamma, \{s_n\}} \quad & \gamma\epsilon + \frac{1}{N} \sum_{n=1}^N s_n \\ \text{s.t.} \quad & s_n \geq \sup_{\mathbf{x} \in \mathcal{X}} \{ \ell_{\text{FY}}(\boldsymbol{\beta}; \mathbf{x}, \mathbf{e}_i) - \gamma \|\mathbf{x} - \mathbf{x}_n\|_{\mathbf{S}} - \gamma \kappa \mathbb{I}(\mathbf{e}_i \neq \mathbf{y}_n) \}, \\ & \forall n \in \{1, \dots, N\}, \forall i \in \{1, \dots, K\}, \\ & \gamma \geq 0. \end{aligned} \quad (46)$$

*Proof.* The proof proceeds in two steps. First, we invoke the strong duality theorem for Wasserstein DRO. Provided the underlying sample space is a Polish space, the transport cost is lower semicontinuous, and the loss is upper semicontinuous and integrably bounded, we can establish the strong duality according to Blanchet and Murthy (2019). In our setting,  $\ell_{\text{FY}}$  is continuous (as shown in Lemma 1) and the hybrid cost is a metric, thereby satisfying these regularity assumptions. Thus, the worst-case risk is exactly given by:

$$\min_{\boldsymbol{\beta}, \gamma \geq 0} \left\{ \gamma\epsilon + \frac{1}{N} \sum_{n=1}^N \sup_{\mathbf{z} \in \mathcal{X} \times \mathcal{Y}} (\ell_{\text{FY}}(\boldsymbol{\beta}; \mathbf{z}) - \gamma c(\mathbf{z}, \mathbf{z}_n)) \right\}.$$

Second, we decompose the supremum over the joint space  $\mathcal{X} \times \mathcal{Y}$ . Since  $\mathcal{Y} = \{\mathbf{e}_1, \dots, \mathbf{e}_K\}$  is a finite discrete set, the global supremum is equivalent to the maximum over  $k$  of the conditional suprema given  $\mathbf{y} = \mathbf{e}_k$ :

$$\sup_{\mathbf{z} \in \mathcal{X} \times \mathcal{Y}} (\dots) = \max_{k \in \{1, \dots, K\}} \sup_{\mathbf{x} \in \mathcal{X}} \{\ell_{\text{FY}}(\boldsymbol{\beta}; \mathbf{x}, \mathbf{e}_i) - \gamma (\|\mathbf{x} - \mathbf{x}_n\|_{\mathbf{S}} + \kappa \mathbb{I}(\mathbf{e}_i \neq \mathbf{y}_n))\}.$$

Substituting this decomposition into the robust constraints for  $s_i$  yields the formulation in (46).

Then, we verify the convexity. The objective function  $\gamma\epsilon + \frac{1}{N} \sum s_n$  is linear in the decision variables  $(\boldsymbol{\beta}, \gamma, \{s_n\})$ , and is therefore convex. Next, consider the inequality constraints defining the feasible set. For each sample  $n$  and label  $k$ , the constraint can be rewritten as  $s_n \geq \phi_{nk}(\boldsymbol{\beta}, \gamma)$ , where

$$\phi_{ni}(\boldsymbol{\beta}, \gamma) := \sup_{\mathbf{x} \in \mathcal{X}} \{\ell_{\text{FY}}(\boldsymbol{\beta}; \mathbf{x}, \mathbf{e}_i) - \gamma \|\mathbf{x} - \mathbf{x}_n\|_{\mathbf{S}}\} - \gamma \kappa \mathbb{I}(\mathbf{e}_i \neq \mathbf{y}_n).$$

We observe that for any fixed  $\mathbf{x} \in \mathcal{X}$ , the term  $\ell_{\text{FY}}(\boldsymbol{\beta}; \mathbf{x}, \mathbf{e}_k)$  is convex in  $\boldsymbol{\beta}$  (due to the convexity of  $\Omega$ ), and the term  $-\gamma(\|\mathbf{x} - \mathbf{x}_n\|_{\mathbf{S}} + \kappa \mathbb{I})$  is linear (and thus convex) in  $\gamma$ . Consequently, the expression inside the supremum is jointly convex with respect to  $(\boldsymbol{\beta}, \gamma)$ . Since the pointwise supremum of a family of convex functions preserves convexity, the function  $\phi_{ni}(\boldsymbol{\beta}, \gamma)$  is jointly convex. The constraints  $s_n \geq \phi_{ni}(\boldsymbol{\beta}, \gamma)$  thus define the epigraphs of convex functions, which are convex sets. Since the intersection of convex sets is convex, the feasible region of (46) is convex. Therefore, the problem minimizes a convex objective over a convex feasible set, characterizing it as a convex optimization problem.  $\square$

Despite the theoretical convexity of the exact reformulation (46), the problem remains computationally prohibitive for general PUMs. The evaluation of the constraint function  $\phi_{ni}(\boldsymbol{\beta}, \gamma)$  necessitates solving the inner maximization problem  $\sup_{\mathbf{x}} \{\ell_{\text{FY}}(\boldsymbol{\beta}; \mathbf{x}, \mathbf{e}_i) - \gamma \|\mathbf{x} - \mathbf{x}_n\|_{\mathbf{S}}\}$ . Since the Fenchel–Young loss  $\ell_{\text{FY}}$  is convex with respect to the feature vector  $\mathbf{x}$ , this inner problem amounts to maximizing a convex function, which is a classic non-convex optimization problem. Consequently, the constraints and their gradients cannot be evaluated efficiently, rendering standard convex solvers inapplicable. To circumvent this intractability, we proceed by deriving a safe convex approximation. In the next section, we utilize the Lipschitz continuity of the loss function to construct a tractable upper bound for the worst-case risk. This approach allows us to replace the implicit and hard-to-compute worst-case constraints with an explicit constraint on the parameter norm, derived from bounding the global Lipschitz constant of the model.

#### 4.2.2 Bounding the Lipschitz Constant with PUM Properties

Recall that for a single observation  $(\mathbf{x}, \mathbf{y})$ , where  $\mathbf{y} \in \{0, 1\}^K$  represents the choice as a one-hot vector, the FY loss is

$$\ell_{\text{FY}}(\boldsymbol{\beta}; \mathbf{x}, \mathbf{y}) = \Omega(\mathbf{V}(\mathbf{x})) - \mathbf{y}^\top \mathbf{V}(\mathbf{x}),$$

where

$$\mathbf{V}(\mathbf{x}) = [V_1(\mathbf{x}), \dots, V_K(\mathbf{x})]^\top, \quad V_i(\mathbf{x}) = \boldsymbol{\beta}^\top \mathbf{x}_i,$$

and  $\mathbf{x} = (\mathbf{x}_1, \dots, \mathbf{x}_K)$  collects the attributes of all alternatives. By the PUM construction,

$$\nabla_{\mathbf{V}} \Omega(\mathbf{V}) = \mathbf{p}(\mathbf{x}; \boldsymbol{\beta}) \in \Delta,$$

so the gradient of the FY loss with respect to  $\mathbf{V}$  is simply the difference between the predicted probability and the label vector:

$$\nabla_{\mathbf{V}} \ell_{\text{FY}} = \nabla_{\mathbf{V}} \Omega(\mathbf{V}) - \mathbf{y} = \mathbf{p}(\mathbf{x}; \boldsymbol{\beta}) - \mathbf{y}.$$

For each alternative  $i$ , the Jacobian of  $\mathbf{V}(\mathbf{x})$  with respect to  $\mathbf{x}_i$  satisfies

$$\nabla_{\mathbf{x}_i} V_j(\mathbf{x}) = \begin{cases} \boldsymbol{\beta}, & j = i, \\ \mathbf{0}, & j \neq i, \end{cases}$$

which yields, by the chain rule,

$$\nabla_{\mathbf{x}_i} \ell_{\text{FY}}(\boldsymbol{\beta}; \mathbf{x}, \mathbf{y}) = (p_i(\mathbf{x}; \boldsymbol{\beta}) - y_i) \boldsymbol{\beta}.$$

Stacking over  $i = 1, \dots, K$ , the gradient with respect to the full feature vector  $\mathbf{x}$  is

$$\nabla_{\mathbf{x}} \ell_{\text{FY}}(\boldsymbol{\beta}; \mathbf{x}, \mathbf{y}) = \left( (p_1 - y_1)\boldsymbol{\beta}, \dots, (p_K - y_K)\boldsymbol{\beta} \right).$$

**Euclidean bound.** The Euclidean norm of this gradient satisfies

$$\begin{aligned} \|\nabla_{\mathbf{x}} \ell_{\text{FY}}(\boldsymbol{\beta}; \mathbf{x}, \mathbf{y})\|_2^2 &= \sum_{i=1}^K (p_i - y_i)^2 \|\boldsymbol{\beta}\|_2^2 \\ &= \|\boldsymbol{\beta}\|_2^2 \|\mathbf{p} - \mathbf{y}\|_2^2. \end{aligned}$$

Since  $\mathbf{p} \in \Delta$  and  $\mathbf{y}$  is a vertex of the simplex (one-hot), we have the simple bound

$$\|\mathbf{p} - \mathbf{y}\|_2^2 = \sum_{i=1}^K (p_i - y_i)^2 = (1 - p_k)^2 + \sum_{j \neq k} p_j^2 \leq (1 - p_k)^2 + (1 - p_k) \leq 2,$$

where  $k$  is the index of the observed class (i.e.,  $y_k = 1$ ). Hence,

$$\|\mathbf{p} - \mathbf{y}\|_2 \leq \sqrt{2}, \quad \|\nabla_{\mathbf{x}} \ell_{\text{FY}}(\boldsymbol{\beta}; \mathbf{x}, \mathbf{y})\|_2 \leq \sqrt{2} \|\boldsymbol{\beta}\|_2. \quad (47)$$

Thus, with respect to the Euclidean norm, the FY loss is  $\sqrt{2} \|\boldsymbol{\beta}\|_2$ -Lipschitz in  $\mathbf{x}$ , for *any* PUM (we only used  $\mathbf{p} \in \Delta$ ).

**Mahalanobis bound.** The DRO formulation uses the Mahalanobis norm  $\|\mathbf{u}\|_{\mathbf{S}} = \sqrt{\mathbf{u}^\top \mathbf{S}^{-1} \mathbf{u}}$ , whose dual norm is

$$\|\mathbf{g}\|_{\mathbf{S},*} := \sup_{\|\mathbf{u}\|_{\mathbf{S}} \leq 1} \mathbf{g}^\top \mathbf{u} = \sqrt{\mathbf{g}^\top \mathbf{S} \mathbf{g}}.$$

By the spectral bound  $\mathbf{g}^\top \mathbf{S} \mathbf{g} \leq \lambda_{\max}(\mathbf{S}) \|\mathbf{g}\|_2^2$ , we obtain

$$\|\nabla_{\mathbf{x}} \ell_{\text{FY}}(\boldsymbol{\beta}; \mathbf{x}, \mathbf{y})\|_{\mathbf{S},*} \leq \sqrt{\lambda_{\max}(\mathbf{S})} \|\nabla_{\mathbf{x}} \ell_{\text{FY}}(\boldsymbol{\beta}; \mathbf{x}, \mathbf{y})\|_2 \leq \sqrt{2 \lambda_{\max}(\mathbf{S})} \|\boldsymbol{\beta}\|_2.$$

Since the Lipschitz constant  $L_{\mathbf{y}}(\boldsymbol{\beta})$  with respect to the Mahalanobis norm is given by

$$L_{\mathbf{y}}(\boldsymbol{\beta}) = \sup_{\mathbf{x} \in \mathcal{X}} \|\nabla_{\mathbf{x}} \ell_{\text{FY}}(\boldsymbol{\beta}; \mathbf{x}, \mathbf{y})\|_{\mathbf{S},*},$$

we may take the uniform bound

$$L(\boldsymbol{\beta}) := \max_{\mathbf{y}} L_{\mathbf{y}}(\boldsymbol{\beta}) \leq \sqrt{2 \lambda_{\max}(\mathbf{S})} \|\boldsymbol{\beta}\|_2. \quad (48)$$

Therefore, substituting the bound in (47) or (48) into the dual constraint  $\gamma \geq L(\boldsymbol{\beta})$ , we may enforce the (slightly stronger) second-order cone constraint

$$\gamma \geq c_{\mathbf{S}} \|\boldsymbol{\beta}\|_2, \quad c_{\mathbf{S}} := \sqrt{2 \lambda_{\max}(\mathbf{S})} \text{ or } \sqrt{2}.$$

### 4.2.3 Tractable Dual Reformulation

We now construct a safe convex approximation. By utilizing the global Lipschitz constant derived above, we replace the implicit local gradient constraints with a uniform upper bound. This relaxation transforms the problem into a computationally efficient finite-dimensional convex optimization problem.

**Theorem 4** (Tractable Reformulation). *Given that the Lipschitz constant for the the map  $\mathbf{x} \mapsto \ell_{\text{FY}}(\boldsymbol{\beta}; \mathbf{x}, \mathbf{e}_i)$  is  $L(\boldsymbol{\beta})$ , the exact distributionally robust problem can be safely approximated by the following finite-dimensional convex optimization problem, which provides an upper bound on the worst-case risk:*

$$\min_{\boldsymbol{\beta}, \gamma, \{s_n\}} \gamma\epsilon + \frac{1}{N} \sum_{n=1}^N s_n \quad (49)$$

subject to

$$\gamma \geq L(\boldsymbol{\beta}), \quad (50)$$

$$s_n \geq \ell_{\text{FY}}(\boldsymbol{\beta}; \mathbf{x}_n, \mathbf{y}_n), \quad \forall n = 1, \dots, N, \quad (51)$$

$$s_n \geq \ell_{\text{FY}}(\boldsymbol{\beta}; \mathbf{x}_n, \mathbf{e}_i) - \gamma\kappa, \quad \forall n = 1, \dots, N, \quad \forall k \text{ such that } \mathbf{e}_i \neq \mathbf{y}_n. \quad (52)$$

*Proof.* We start from the exact semi-infinite reformulation derived in Theorem 3, specifically Equation (46). The constraints require that for every sample  $i$  and class  $k$ :

$$s_n \geq \sup_{\mathbf{x} \in \mathcal{X}} \{\ell_{\text{FY}}(\boldsymbol{\beta}; \mathbf{x}, \mathbf{e}_i) - \gamma\|\mathbf{x} - \mathbf{x}_n\|_{\mathbf{S}}\} - \gamma\kappa\mathbb{I}(\mathbf{e}_i \neq \mathbf{y}_n). \quad (53)$$

The inner maximization problem involves the convex loss function and is generally intractable. To construct a tractable upper bound, we utilize the Lipschitz continuity of the loss. By the definition of the Lipschitz constant  $L(\boldsymbol{\beta})$ , we have the inequality:

$$\ell_{\text{FY}}(\boldsymbol{\beta}; \mathbf{x}, \mathbf{e}_i) \leq \ell_{\text{FY}}(\boldsymbol{\beta}; \mathbf{x}_n, \mathbf{e}_i) + L(\boldsymbol{\beta})\|\mathbf{x} - \mathbf{x}_n\|_{\mathbf{S}}. \quad (54)$$

Substituting this upper bound into the supremum yields:

$$\sup_{\mathbf{x} \in \mathcal{X}} \{\ell_{\text{FY}}(\boldsymbol{\beta}; \mathbf{x}, \mathbf{e}_i) - \gamma\|\mathbf{x} - \mathbf{x}_n\|_{\mathbf{S}}\} \leq \ell_{\text{FY}}(\boldsymbol{\beta}; \mathbf{x}_n, \mathbf{e}_i) + \sup_{\mathbf{x} \in \mathcal{X}} \{(L(\boldsymbol{\beta}) - \gamma)\|\mathbf{x} - \mathbf{x}_n\|_{\mathbf{S}}\}. \quad (55)$$

If we enforce the constraint  $\gamma \geq L(\boldsymbol{\beta})$ , the term  $(L(\boldsymbol{\beta}) - \gamma)$  is non-positive. Consequently, the supremum over the unbounded domain  $\mathcal{X}$  is attained at  $\mathbf{x} = \mathbf{x}_n$  (where the norm is zero), and the term vanishes. Conversely, if  $\gamma < L(\boldsymbol{\beta})$ , the supremum explodes to  $+\infty$ , making the minimization over  $\gamma$  infeasible or suboptimal.

Therefore, by restricting the search space to  $\gamma \geq L(\boldsymbol{\beta})$ , we can replace the intractable supremum with the nominal loss value:

$$\sup_{\mathbf{x} \in \mathcal{X}} \{\ell_{\text{FY}}(\boldsymbol{\beta}; \mathbf{x}, \mathbf{e}_i) - \gamma\|\mathbf{x} - \mathbf{x}_n\|_{\mathbf{S}}\} \leq \ell_{\text{FY}}(\boldsymbol{\beta}; \mathbf{x}_n, \mathbf{e}_i). \quad (56)$$

Applying this relaxation to the constraints in (46) for both the correct label case ( $\mathbf{e}_i = \mathbf{y}_n$ , where the indicator is 0) and the incorrect label case ( $\mathbf{e}_i \neq \mathbf{y}_n$ , where the indicator is 1) directly yields the finite system of constraints (50)–(52). Since the feasible set of this approximate problem is a subset of the exact problem’s feasible set (due to the upper bound on the  $s_n$  constraints), the optimal value provides an upper bound on the true worst-case risk, making it a safe approximation.  $\square$

By substituting the explicit Lipschitz constant derived above (i.e.,  $L(\boldsymbol{\beta}) = c_{\mathbf{S}}\|\boldsymbol{\beta}\|_2$ ), the problem admits the explicit formulation:

$$\begin{aligned}
\min_{\boldsymbol{\beta}, \gamma, \{s_n\}} \quad & \gamma\epsilon + \frac{1}{N} \sum_{n=1}^N s_n \\
\text{s.t.} \quad & s_n \geq \ell_{\text{FY}}(\boldsymbol{\beta}; \mathbf{x}_n, \mathbf{y}_n), \quad n = 1, \dots, N, \\
& s_n \geq \ell_{\text{FY}}(\boldsymbol{\beta}; \mathbf{x}_n, \mathbf{e}_i) - \gamma\kappa, \quad n = 1, \dots, N, \forall k \text{ s.t. } \mathbf{e}_i \neq \mathbf{y}_n, \\
& \gamma \geq c_{\mathbf{S}} \|\boldsymbol{\beta}\|_2.
\end{aligned} \tag{57}$$

Since  $\ell_{\text{FY}}(\boldsymbol{\beta}; \mathbf{x}, \mathbf{y})$  is convex in  $\boldsymbol{\beta}$  and the constraint  $\gamma \geq c_{\mathbf{S}}\|\boldsymbol{\beta}\|_2$  defines a convex second-order cone, the problem (57) is a globally convex optimization problem. It can be solved efficiently using standard conic solvers or first-order methods, where the distributionally robust formulation effectively adds a geometry-aware norm regularization to the standard Fenchel–Young loss.

#### 4.2.4 Solution Algorithm for the Tractable Approximation

While the tractable reformulation derived in Theorem 4 constitutes a valid second-order cone program that can be solved via interior-point methods, it contains inner optimization problems (i.e., solving  $\ell_{\text{FY}}(\boldsymbol{\beta}; \mathbf{x}_n, \mathbf{y}_n)$ ) in the constraints. To enable efficient large-scale estimation, we propose a first-order primal-dual algorithm by restructuring the problem into a convex-concave saddle point formulation. Recall that the robustified loss function essentially involves the surplus function  $\Omega(\mathbf{V})$ . By invoking the variational definition  $\Omega(\mathbf{V}) = \sup_{\mathbf{p} \in \Delta} \{\mathbf{p}^\top \mathbf{V} - \Lambda(\mathbf{p})\}$ , we can lift the implicit probability vectors to explicit dual optimization variables. Consequently, the minimization of the robust objective is equivalent to the following minimax problem:

$$\min_{\substack{\boldsymbol{\beta} \in \mathbb{R}^d, \gamma \in \mathbb{R} \\ \gamma \geq c_{\mathbf{S}}\|\boldsymbol{\beta}\|_2}} \max_{\mathbf{p}^\circ \in \Delta^N} \mathcal{L}(\boldsymbol{\beta}, \gamma, \mathbf{p}^\circ) := \gamma\epsilon + \frac{1}{N} \sum_{n=1}^N \left[ \underbrace{\mathbf{p}_n^\top \mathbf{V}(\mathbf{x}_n; \boldsymbol{\beta}) - \Lambda(\mathbf{p}_n)}_{\text{Variational form of } \Omega(\mathbf{V}_n)} + \mathcal{R}_n(\boldsymbol{\beta}, \gamma) \right], \tag{58}$$

where  $\mathbf{p}^\circ = (\mathbf{p}_1, \dots, \mathbf{p}_N)$  denotes the collection of dual probability vectors, and  $\mathcal{R}_n(\boldsymbol{\beta}, \gamma)$  represents the adversarial correction term derived from the finite constraints:

$$\mathcal{R}_n(\boldsymbol{\beta}, \gamma) := \max_{i \in \{1, \dots, K\}} \left\{ -\mathbf{e}_i^\top \mathbf{V}(\mathbf{x}_n; \boldsymbol{\beta}) - \mathbb{I}(\mathbf{e}_i \neq \mathbf{y}_n) \gamma \kappa \right\}. \tag{59}$$

The saddle point formulation presented in Eq. (58) involves the term  $\mathcal{R}_n(\boldsymbol{\beta}, \gamma)$ , which is defined as the pointwise maximum of a finite set of affine functions. Consequently, the objective function is non-smooth with respect to the primal variables  $\boldsymbol{\beta}$  and  $\gamma$ , as the gradient is undefined at points where multiple indices  $k$  achieve the maximum simultaneously. To circumvent this issue and recover a fully smooth objective, we can further dualize the discrete maximization by introducing an auxiliary adversarial probability vector  $\mathbf{q}_n \in \Delta_K$  for each sample. By exploiting the variational identity  $\max_i \{z_i\} = \max_{\mathbf{q} \in \Delta_K} \mathbf{q}^\top \mathbf{z}$ , we transform the non-smooth piecewise linear term into a smooth bilinear term. This leads to the following bilinear saddle point problem:

$$\min_{\substack{\boldsymbol{\beta} \in \mathbb{R}^d, \gamma \in \mathbb{R} \\ \gamma \geq c_{\mathbf{S}}\|\boldsymbol{\beta}\|_2}} \max_{\substack{\mathbf{p}^\circ \in \Delta^N \\ \mathbf{q}^\circ \in \Delta^N}} \mathcal{L}_{\text{bilinear}}(\boldsymbol{\beta}, \gamma, \mathbf{p}^\circ, \mathbf{q}^\circ), \tag{60}$$

where  $\mathbf{q}^\circ = (\mathbf{q}_1, \dots, \mathbf{q}_N)$  denotes the collection of adversarial label distributions. The smoothed objective function is given by:

$$\begin{aligned} \mathcal{L}_{\text{bilinear}} &:= \frac{1}{N} \sum_{n=1}^N \left[ (\mathbf{p}_n - \mathbf{q}_n)^\top \mathbf{V}(\mathbf{x}_n; \boldsymbol{\beta}) - \Lambda(\mathbf{p}_n) \right] \\ &\quad + \gamma \left( \epsilon - \frac{\kappa}{N} \sum_{n=1}^N \sum_{i=1}^K q_{ni} \mathbb{I}(\mathbf{e}_i \neq \mathbf{y}_n) \right). \end{aligned} \quad (61)$$

The mathematical structure of Eq. (60) is favorable for numerical optimization. Specifically, the objective function  $\mathcal{L}_{\text{bilinear}}$  is *convex-concave*: it is affine (and thus convex) with respect to the primal variables  $(\boldsymbol{\beta}, \gamma)$ , and concave with respect to the dual variables  $(\mathbf{p}^\circ, \mathbf{q}^\circ)$ . Notably, the strict convexity of the regularizer  $\Lambda$  implies that the objective is strictly concave in  $\mathbf{p}^\circ$ , ensuring the uniqueness of the optimal prediction distribution.

Furthermore, unlike the original formulation involving the pointwise maximum, this bilinear formulation is smooth with Lipschitz continuous gradients. Combined with the fact that the constraints, i.e., the second-order cone for the primal variables and the probability simplexes for the dual variables, are simple convex sets admitting efficient closed-form projections, this problem can be solved efficiently using the projected extragradient algorithm, as demonstrated in Section 3.5. In algorithmic practice, to further enhance convergence stability and mitigate potential oscillatory behavior inherent in min-max optimization, a two-time-scale strategy can be incorporated into this framework (Lin et al., 2025), i.e., setting a longer step size for the inner iteration than the outer iteration.

### 4.3 Equivalences of the Tractable Reformulation in Two Limiting Cases

Recall that the basic (non-robust) Fenchel–Young estimator is obtained by minimizing the empirical Fenchel–Young loss:

$$\min_{\boldsymbol{\beta}} \mathcal{J}_{\text{FY}}(\boldsymbol{\beta}) := \frac{1}{N} \sum_{n=1}^N \ell(\boldsymbol{\beta}; \mathbf{x}_n, \mathbf{y}_n). \quad (62)$$

In contrast, utilizing the tractable reformulation derived in Theorem 4, the Wasserstein DRO problem is approximated by the finite-dimensional dual problem (57). Critically, this formulation relies on the global Lipschitz upper bound  $c_{\mathbf{S}}$  (derived from the PUM structure and the Mahalanobis metric) to replace the intractable local gradient constraints of the exact formulation.

For any fixed pair  $(\boldsymbol{\beta}, \gamma)$ , the optimal slack variables are given by

$$s_n^*(\boldsymbol{\beta}, \gamma) = \max \left\{ \ell(\boldsymbol{\beta}; \mathbf{x}_n, \mathbf{y}_n), \max_{\mathbf{e}_k \neq \mathbf{y}_n} [\ell(\boldsymbol{\beta}; \mathbf{x}_n, \mathbf{e}_k) - \gamma \kappa] \right\}, \quad (63)$$

where the inner maximization is taken over all alternative choice vectors  $\mathbf{e}_k$  distinct from the observed choice  $\mathbf{y}_n$ . Substituting  $s_n^*$  into (57), the tractable DRO problem can be written purely in terms of  $(\boldsymbol{\beta}, \gamma)$  as

$$\min_{\boldsymbol{\beta}, \gamma} \quad \gamma \epsilon + \frac{1}{N} \sum_{n=1}^N \tilde{\ell}_{\text{DRO}}(\boldsymbol{\beta}, \gamma; \mathbf{x}_n, \mathbf{y}_n) \quad \text{s.t.} \quad \gamma \geq c_{\mathbf{S}} \|\boldsymbol{\beta}\|_2, \quad (64)$$

where the *robustified* per-sample loss is defined as

$$\tilde{\ell}_{\text{DRO}}(\boldsymbol{\beta}, \gamma; \mathbf{x}_n, \mathbf{y}_n) := \max \left\{ \ell(\boldsymbol{\beta}; \mathbf{x}_n, \mathbf{y}_n), \max_{\mathbf{e}_i \neq \mathbf{y}_n} [\ell(\boldsymbol{\beta}; \mathbf{x}_n, \mathbf{e}_i) - \gamma \kappa] \right\}. \quad (65)$$

Therefore, the Wasserstein–DRO estimator can be interpreted as a *twofold modification* of the basic Fenchel–Young formulation (62). First, the empirical FY loss for each observation is replaced by the worst-case loss over adversarial label perturbations, penalized by  $\gamma\kappa$ ; this inflates the objective whenever alternative choice vectors ( $\mathbf{e}_i$ ) can explain the data almost as well as the observed vector ( $\mathbf{y}_n$ ). Second, the constraint  $\gamma \geq c_S \|\boldsymbol{\beta}\|_2$  together with the term  $\gamma\epsilon$  induces an implicit norm-regularization on  $\boldsymbol{\beta}$ , whose strength is controlled by the Wasserstein radius  $\epsilon$ . In this sense, the DRO formulation is equivalent to minimizing a robustified Fenchel–Young loss plus a distributional-uncertainty-driven penalty on the magnitude of the utility coefficients.

### 4.3.1 Limiting Case: The Regularization Equivalence

We now turn our attention to the specific asymptotic regime where the penalty for label flipping becomes prohibitively large, i.e.,  $\kappa \rightarrow \infty$ . This regime corresponds to a modeling scenario where the analyst places absolute trust in the observed discrete choices (represented by one-hot vectors  $\mathbf{y}_n$ ) but acknowledges the potential measurement errors or unobserved heterogeneity in the attributes (features  $\mathbf{x}_n$ ).

As  $\kappa \rightarrow \infty$ , the adversarial term  $\ell(\boldsymbol{\beta}; \mathbf{x}_n, \mathbf{e}_i) - \gamma\kappa$  tends to  $-\infty$  for any finite dual variable  $\gamma > 0$  and any alternative choice vector  $\mathbf{e}_i \neq \mathbf{y}_n$ . Consequently, the maximization over the alternative choices becomes inactive, as the adversary cannot afford the infinite cost of falsifying the observed choice. Mathematically, the robustified loss function collapses to the nominal loss:

$$\lim_{\kappa \rightarrow \infty} \tilde{\ell}_{\text{DRO}}(\boldsymbol{\beta}, \gamma; \mathbf{x}_n, \mathbf{y}_n) = \ell(\boldsymbol{\beta}; \mathbf{x}_n, \mathbf{y}_n). \quad (66)$$

In this limit, the auxiliary variables  $s_i$  are constrained solely by the nominal Fenchel–Young loss. The optimization problem (64) simplifies to minimizing  $\gamma\epsilon + \frac{1}{N} \sum \ell(\boldsymbol{\beta}; \mathbf{x}_n, \mathbf{y}_n)$  subject to the gradient norm constraint  $\gamma \geq c_S \|\boldsymbol{\beta}\|_2$ .

Since the objective function is monotone increasing in  $\gamma$ , and  $\epsilon$  represents a positive uncertainty budget, the optimal dual variable  $\gamma^*$  must bind at its lower bound to minimize the objective. Thus, at optimality, we have:

$$\gamma^* = c_S \|\boldsymbol{\beta}\|_2. \quad (67)$$

Substituting this optimal  $\gamma^*$  back into the objective function yields a reduced-form estimator, which is presented in the following theorem.

**Theorem 5** (Limiting Equivalence to  $\ell_2$ -Regularization). *Consider the Wasserstein Distributionally Robust Optimization problem formulated in (64) with the hybrid transport cost. In the asymptotic regime where the label mismatch penalty  $\kappa \rightarrow \infty$ , the robust estimator is characterized as the solution to the following  $\ell_2$ -regularized Empirical Risk Minimization problem:*

$$\hat{\boldsymbol{\beta}}_{\kappa \rightarrow \infty} \in \arg \min_{\boldsymbol{\beta}} \left\{ \underbrace{\frac{1}{N} \sum_{i=n}^N \ell_{\text{FY}}(\boldsymbol{\beta}; \mathbf{x}_n, \mathbf{y}_n)}_{\text{Empirical Risk}} + \underbrace{\lambda_{\text{reg}} \|\boldsymbol{\beta}\|_2}_{\text{Regularization}} \right\}, \quad (68)$$

where the regularization coefficient is explicitly determined by the ambiguity set radius  $\epsilon$  and the geometric Lipschitz constant  $c_S$  via the relation  $\lambda_{\text{reg}} := \epsilon c_S$ .

This theorem elucidates a fundamental duality implied by the tractable DRO formulation: robustness against feature perturbations (under the Lipschitz approximation) is mathematically

equivalent to norm-regularization in the parameter space. The term  $\epsilon$  controls the radius of the uncertainty ball in the feature space, which translates directly into the strength of the shrinkage penalty  $\lambda_{\text{reg}}$  applied to the utility parameters.

Furthermore, the presence of the constant  $c_S$  (derived from the Mahalanobis metric) highlights the adaptive nature of this regularization. Unlike standard Ridge regression which applies isotropic shrinkage, the DRO-derived regularization is geometry-aware: it penalizes the parameter magnitude more heavily in directions where the data variance (and thus the potential for adversarial perturbation) is larger.

In summary, the general Wasserstein–DRO formulation proposed in this paper encapsulates the standard regularized estimator as a special limiting case, which resonates the results stated in Blanchet and Murthy (2019). However, by allowing for a finite  $\kappa$ , our formulation provides a richer class of estimators that simultaneously perform *parameter shrinkage* (via  $\gamma$ ) to combat high variance and *loss truncation* (via  $\kappa$ ) to robustify against outliers and perfect separation.

### 4.3.2 Limiting Case: The Hinge Loss Equivalence

In this specific limiting instance, we consider the regime where both the label mismatch penalty  $\kappa$  and the Wasserstein ambiguity radius  $\epsilon$  approach zero simultaneously ( $\kappa \rightarrow 0, \epsilon \rightarrow 0$ ), while their magnitudes remain comparable. Under this asymptotic condition, the geometric structure of the ambiguity set  $\mathbb{B}_\epsilon(\hat{\mathbb{P}}_N)$  undergoes a fundamental transformation regarding the hybrid transport cost. Since the radius  $\epsilon$  becomes infinitesimal, the allowable budget for transporting probability mass across the continuous feature space effectively vanishes. Consequently, the decision-maker implicitly assumes near-perfect reliability of the observed attributes  $\mathbf{x}$ , as the cost of perturbing features exceeds the tight uncertainty budget. The effective coverage of the Wasserstein ball is thus restricted almost exclusively to the discrete label space. In this regime, the robustness mechanism decouples from the feature geometry (eliminating the parameter shrinkage effect linked to  $\|\boldsymbol{\beta}\|_2$ ) and focuses entirely on the discrete adversarial perturbations.

Based on the robustified loss formulation in Eq. (64), as both  $\epsilon$  and  $\kappa$  tend to zero, a non-trivial equilibrium requires the dual variable  $\gamma$  to grow sufficiently large to counterbalance the vanishing penalty  $\kappa$ . Specifically, for the adversarial term  $\ell(\boldsymbol{\beta}; \mathbf{x}_i, \mathbf{e}_k) - \gamma\kappa$  to remain active and meaningful, the product  $\gamma\kappa$  must converge to a finite constant. This implies  $\gamma \rightarrow \infty$ , rendering the gradient norm constraint  $\gamma \geq c_S\|\boldsymbol{\beta}\|_2$  asymptotically inactive (slack), thereby decoupling the dual variable from the parameter magnitude. By defining the effective hinged threshold  $\tau = \gamma\kappa$ , the regularization term transforms as  $\gamma\epsilon = \tau(\epsilon/\kappa)$ . Consequently, the DRO problem (64) can be reformulated as a hierarchical two-level optimization: an outer optimization over the global threshold  $\tau$  (weighted by the ratio  $\epsilon/\kappa$ ), and an inner unconstrained minimization over  $\boldsymbol{\beta}$  using a pure truncated loss function:

$$\min_{\tau \geq 0} \left\{ \frac{\epsilon}{\kappa} \tau + \min_{\boldsymbol{\beta}} \left[ \frac{1}{N} \sum_{n=1}^N \max \left( \ell(\boldsymbol{\beta}; \mathbf{x}_n, \mathbf{y}_n), \max_{\mathbf{e}_i \neq \mathbf{y}_n} \{ \ell(\boldsymbol{\beta}; \mathbf{x}_n, \mathbf{e}_i) - \tau \} \right) \right] \right\} \quad (69)$$

The inner minimization problem functions as an *adversarial margin enforcement* mechanism. Governed by the pointwise maximum operator  $\max(\ell_{\text{real}}, \ell_{\text{adv}} - \tau)$ , the optimization objective dynamically adapts to the classification quality of each sample. For “easy” samples where the model predicts the true label with high confidence—resulting in a negligible nominal loss  $\ell(\boldsymbol{\beta}; \mathbf{x}_n, \mathbf{y}_n)$  but a large adversarial loss—the objective switches to the adversarial component  $\max_{\mathbf{e}_i \neq \mathbf{y}_n} \{ \ell(\boldsymbol{\beta}; \mathbf{x}_n, \mathbf{e}_i) - \tau \}$ . This prevents the optimizer from settling for mere correctness; instead, it compels the model to further suppress the utility of competitive incorrect classes, thereby enforcing a robust safety margin  $\tau$ . Conversely, for “hard” samples or outliers where the model misclassifies the data (yielding a large

nominal loss), the operator retains the nominal loss to prioritize error correction. Mathematically, this mirrors a generalized multi-class Hinge loss, ensuring the decision boundary is regularized by strictly separated confidence intervals while maintaining sensitivity to significant errors.

The outer optimization over the scalar variable  $\tau$  effectively searches for the globally optimal safety margin. By minimizing the aggregate objective, this step balances the empirical margin violations from the inner problem against the linear penalty weighted by the ratio  $\epsilon/\kappa$ . This structural insight naturally leads to the following theorem, which formally characterizes the estimator in this limiting regime.

**Theorem 6** (Limiting Equivalence to Margin-Optimized Hinge Loss). *Consider the asymptotic regime where the label mismatch penalty  $\kappa$  and the Wasserstein ambiguity radius  $\epsilon$  vanish simultaneously, i.e.,  $\kappa \rightarrow 0$  and  $\epsilon \rightarrow 0$ , such that their ratio converges to a finite constant  $\nu := \lim(\epsilon/\kappa) > 0$ . Under this condition, the distributional robustness with respect to the hybrid transport cost degenerates into a pure label-uncertainty problem. Consequently, the Wasserstein distributionally robust estimator  $\hat{\beta}_{\text{DRO}}$  is characterized as the solution to the following bilevel convex optimization problem:*

$$\hat{\beta}_{\text{DRO}} \in \arg \min_{\beta} \left\{ \min_{\tau \geq 0} \left( \nu\tau + \frac{1}{N} \sum_{n=1}^N \max \left\{ \ell_{\text{FY}}(\beta; \mathbf{x}_n, \mathbf{y}_n), \max_{\mathbf{e}_i \neq \mathbf{y}_n} (\ell_{\text{FY}}(\beta; \mathbf{x}_n, \mathbf{e}_i) - \tau) \right\} \right) \right\}. \quad (70)$$

Here, the inner optimization minimizes a generalized multi-class Hinge loss with a dynamic safety margin  $\tau$ , while the outer optimization determines the globally optimal margin  $\tau^*$  by balancing the empirical margin violations against the linear penalty  $\nu\tau$ .

In practical optimization scenarios where the specific ratio  $\nu = \epsilon/\kappa$  is a priori uncertain or treated as a hyperparameter, varying  $\nu$  is mathematically equivalent to sweeping across different values of the safety margin  $\tau$ . Consequently, rather than solving the full bilevel optimization for a fixed  $\nu$ , one can treat  $\tau$  directly as a tunable hyperparameter. In this context, it suffices to solve the inner minimization problem for a range of candidate  $\tau$  values, thereby generating a regularization path of estimators that enforce varying degrees of adversarial margin.

#### 4.4 Determining the Wasserstein Radius

In this subsection, we establish a theoretical guideline for selecting the Wasserstein radius  $\epsilon$ , which is the critical hyperparameter in our distributionally robust framework. To isolate the impact of distributional uncertainty in the feature space, we focus on the regime where the label flipping penalty is prohibitively large (i.e.,  $\kappa \rightarrow \infty$ ). As established in Eq. (65), the DRO formulation in this limit is equivalent to the standard regularized Fenchel-Young estimator:

$$\hat{\beta}_{\lambda} = \arg \min_{\beta} \{ \mathcal{J}(\beta) + \lambda \|\beta\|_2 \}, \quad (71)$$

where  $\mathcal{J}(\beta) := \frac{1}{N} \sum_n \ell_{\text{FY}}(\beta; \mathbf{x}_n, \mathbf{y}_n)$  is the empirical risk, and the regularization coefficient is directly proportional to the radius:  $\lambda = \epsilon c_{\mathbf{S}}$ .

We first analyze the geometric sensitivity of the estimator to the regularization strength. The following lemma demonstrates that, under standard regularity conditions, the displacement of the estimator from the nominal solution is locally linear with respect to the regularization coefficient (and consequently, the Wasserstein radius).

**Lemma 3** (Linear Sensitivity of the Regularized Estimator). *Let  $\hat{\beta}_0$  be the minimizer of the unregularized empirical risk  $\mathcal{J}(\beta)$  and assume  $\hat{\beta}_0 \neq \mathbf{0}$ . Assume that  $\mathcal{J}$  is twice continuously*

differentiable in a neighborhood of  $\hat{\beta}_0$  and that the empirical Hessian matrix  $\mathbf{H}_N := \nabla^2 \mathcal{J}(\hat{\beta}_0)$  is positive definite. Then, for a sufficiently small regularization coefficient  $\lambda > 0$ , the distance between the robust estimator  $\hat{\beta}_\lambda$  and the nominal estimator  $\hat{\beta}_0$  satisfies:

$$\|\hat{\beta}_\lambda - \hat{\beta}_0\|_2 \approx \lambda \cdot \|\mathbf{H}_N^{-1} \mathbf{u}\|_2, \quad (72)$$

where  $\mathbf{u} = \hat{\beta}_0 / \|\hat{\beta}_0\|_2$  is the unit direction vector of the parameters. Consequently, the estimation bias induced by the Wasserstein constraint is approximately proportional to the radius  $\epsilon$ :

$$\|\hat{\beta}_\epsilon - \hat{\beta}_0\|_2 \propto \epsilon. \quad (73)$$

*Proof.* The first-order optimality condition for the regularized problem is given by:

$$\nabla \mathcal{J}(\hat{\beta}_\lambda) + \lambda \frac{\hat{\beta}_\lambda}{\|\hat{\beta}_\lambda\|_2} = \mathbf{0}. \quad (74)$$

Consider the first-order Taylor expansion of the gradient  $\nabla \mathcal{J}$  around the unregularized minimizer  $\hat{\beta}_0$ . Noting that  $\nabla \mathcal{J}(\hat{\beta}_0) = \mathbf{0}$ , we have:

$$\nabla \mathcal{J}(\hat{\beta}_\lambda) \approx \mathbf{H}_N(\hat{\beta}_\lambda - \hat{\beta}_0). \quad (75)$$

Substituting this into the optimality condition yields:

$$\mathbf{H}_N(\hat{\beta}_\lambda - \hat{\beta}_0) \approx -\lambda \frac{\hat{\beta}_\lambda}{\|\hat{\beta}_\lambda\|_2}. \quad (76)$$

For small  $\lambda$ , the direction of the estimator does not change abruptly, so we approximate  $\hat{\beta}_\lambda / \|\hat{\beta}_\lambda\|_2 \approx \hat{\beta}_0 / \|\hat{\beta}_0\|_2 =: \mathbf{u}$ . Solving for the displacement gives:

$$\hat{\beta}_\lambda - \hat{\beta}_0 \approx -\lambda \mathbf{H}_N^{-1} \mathbf{u}. \quad (77)$$

Taking the Euclidean norm on both sides completes the proof.  $\square$

The Lemma above establishes that the Wasserstein radius  $\epsilon$  acts as a linear control knob for the magnitude of the estimator's displacement from the empirical minimizer. The remaining question is: how much displacement is optimal?

From a statistical learning perspective, the goal of regularization is to counteract the variance of the estimator inherent to finite sampling. The regularization strength should therefore be calibrated to the magnitude of the natural estimation error. If  $\epsilon$  is too small, it fails to stabilize the high-variance components; if  $\epsilon$  is too large, it introduces excessive bias that overwhelms the true signal.

Based on the asymptotic normality of Fenchel-Young estimators (Theorem 2), we derive the optimal scaling law for the Wasserstein radius with respect to the sample size  $N$  and the parameter dimension  $d$ .

**Proposition 5** (Optimal Scaling of the Wasserstein Radius). *Consider a well-specified PUM with a true parameter vector  $\beta^* \in \mathbb{R}^d$ . Let  $\hat{\beta}_0$  denote the unregularized empirical estimator based on  $N$  independent samples. Under the regularity conditions of Theorem 2, the expected Euclidean estimation error due to variance scales as  $\mathcal{O}(\sqrt{d/N})$ .*

*To effectively mitigate this finite-sample error (variance) while minimizing the introduction of systematic bias, the optimal Wasserstein radius  $\epsilon$  should be chosen proportional to the inverse Signal-to-Noise Ratio:*

$$\epsilon \propto \frac{1}{\|\beta^*\|_2} \sqrt{\frac{d}{N}}. \quad (78)$$

*Proof.* The derivation relies on matching the regularization strength to the optimal bias-variance trade-off characterizing the asymptotic regime.

First, consider the variance. According to Theorem 2, the unregularized estimator exhibits asymptotic normality, implying that the estimation error due to finite-sample variance scales as:

$$\mathbb{E} \left[ \|\hat{\beta}_0 - \beta^*\|_2 \right] \sim \mathcal{O} \left( \sqrt{\frac{d}{N}} \right). \quad (79)$$

Second, consider the bias. Lemma 3 establishes that the Wasserstein radius  $\epsilon$  induces a linear displacement (bias) of magnitude  $\|\hat{\beta}_\epsilon - \hat{\beta}_0\|_2 \propto \epsilon$ . To achieve statistical optimality (i.e., minimal Mean Squared Error), this induced bias must be calibrated to counteract the variance effectively.

We draw an analogy to the theory of optimal shrinkage (e.g., Ridge regression or James-Stein estimation). In standard Ridge regression with a quadratic penalty  $\lambda_{\text{Ridge}} \|\beta\|_2^2$ , the optimal regularization parameter is known to scale inversely with the signal energy:  $\lambda_{\text{Ridge}}^* \propto d / \|\beta^*\|_2^2$ . The effective “shrinkage force” exerted by this optimal quadratic penalty on the parameter vector is given by the gradient magnitude:  $\|\nabla(\lambda_{\text{Ridge}}^* \|\beta\|_2^2)\| = 2\lambda_{\text{Ridge}}^* \|\beta\|_2 \propto 1 / \|\beta^*\|_2$ .

In our limiting DRO formulation, the penalty is linear in the norm ( $\lambda \|\beta\|_2$ ), exerting a constant shrinkage force of magnitude  $\lambda = \epsilon c_S$ . Equating the DRO shrinkage force to the optimal Ridge shrinkage force yields the scaling law for the regularization coefficient:

$$\epsilon c_S \propto \frac{1}{\|\beta^*\|_2}. \quad (80)$$

Finally, incorporating the sample-size dependence of the noise level (which dictates the scale of the required correction), the optimal radius must decay with the accumulation of evidence. Following standard concentration results for Wasserstein balls which suggest a radius scaling of  $\mathcal{O}(\sqrt{d/N})$  to cover the true distribution, and modulating this by the signal-to-noise intensity derived above, we arrive at the unified scaling law:

$$\epsilon \propto \frac{1}{\|\beta^*\|_2} \sqrt{\frac{d}{N}}. \quad (81)$$

□

This proposition refines the practical guidelines for hyperparameter tuning by explicitly incorporating the *model signal strength*. While the radius should decay with the square root of the sample size ( $\sqrt{N}$ ) and grow with model complexity ( $\sqrt{d}$ ), it is inversely related to the magnitude of the utility parameters ( $\|\beta^*\|_2$ ). Intuitively, this reflects a Signal-to-Noise adaptation: when parameters are small (weak signal), the empirical risk landscape is flat and susceptible to noise, requiring a larger Wasserstein radius (stronger robustness) to stabilize the estimator. Conversely, when parameters are large (strong signal), the choice probabilities are distinct, and the estimator naturally requires less regularization.

## 5 Numerical Studies

In this section, we present a comprehensive series of numerical experiments designed to empirically validate the theoretical framework established in the preceding chapters. The primary objective is to demonstrate the practical efficacy and computational behavior of the proposed estimation methods through specific computational examples. The section is organized into three distinct parts. The first subsection tests the convergence performance of the proposed algorithm. The second subsection

utilizes synthetic datasets generated under controlled conditions to systematically investigate the finite-sample performance of the Fenchel-Young estimator. In this context, we place particular emphasis on the Wasserstein DRO formulation, analyzing its numerical properties and verifying its capacity to mitigate finite-sample bias as predicted by theory. In the third subsection, we transition to an empirical application using the Swissmetro dataset, a canonical benchmark in discrete choice analysis. This real-world case study allows us to rigorously test the proposed robust models against standard specifications, assessing their estimation stability and predictive accuracy in a practical transportation planning scenario.

### 5.1 Testing the Solution Algorithms

In this subsection, we evaluate the computational performance and convergence properties of the proposed solution algorithms for PUM estimation featuring non-separable perturbation functions. Specifically, we test the optimization algorithms designed for both the standard Fenchel-Young estimator and the tractable saddle-point reformulation of the Wasserstein DRO estimator, which employs the Projected Extragradient method. To assess the algorithms beyond the standard additive separable cases, we construct a non-separable quadratic regularizer. This is operationalized by defining a strictly positive definite matrix  $\mathbf{Q} \in \mathbb{R}^{m \times m}$ , generated as  $\mathbf{Q} = \mathbf{K}^\top \mathbf{K} + \mathbf{I}_m$ , where  $\mathbf{K}$  is a random matrix with entries drawn from a standard normal distribution, and  $\mathbf{I}_m$  is the identity matrix. The corresponding perturbation function takes the form  $\Lambda(\mathbf{p}) = \frac{\mu}{2} \mathbf{p}^\top \mathbf{Q} \mathbf{p}$ , introducing complex cross-alternative correlations that challenge the optimization process.

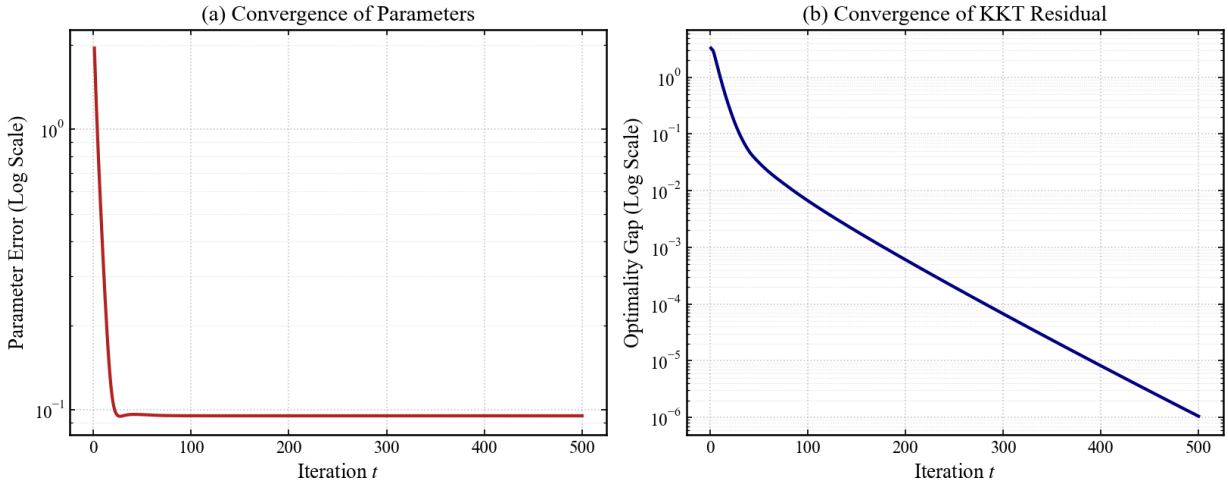


Figure 2: Convergence performance of the Projected Extragradient algorithm for the standard Fenchel-Young estimator under a non-separable quadratic perturbation. Panel (a) illustrates the rapid stabilization of the parameter error in Euclidean distance. Panel (b) demonstrates the monotonic decrease of the KKT residual on a logarithmic scale. The algorithm achieves linear convergence in this scenario.

Figure 2 illustrates the convergence behavior of the Fenchel-Young estimator using the Projected Extragradient algorithm. The numerical experiment is conducted on a large-scale problem featuring a 10-dimensional parameter space, 10 discrete alternatives, and 5,000 observations. Remarkably, the algorithm completes 500 iterations in merely 0.77 seconds, demonstrating the exceptional computational efficiency and stability of the PEG method for such problem scales. To quantitatively assess the optimality, the KKT residual is computed as the norm of the gradient mapping, i.e., the

Euclidean distance between the current primal-dual variables and their projected states following a gradient step, normalized by the respective step sizes. Panel (b) confirms the strict monotonic decrease of this KKT residual, validating the theoretical convergence of the saddle-point formulation. However, as observed in Panel (a), the parameter error relative to the true data-generating parameters is not strictly monotonically decreasing. This phenomenon occurs because the empirical risk minimizer, derived from a finite sample of 5,000 observations, inherently deviates from the true population parameters due to sampling noise. Consequently, the optimization trajectory may temporarily traverse regions in the parameter space that are closer to the true values before ultimately settling at the empirical optimum.

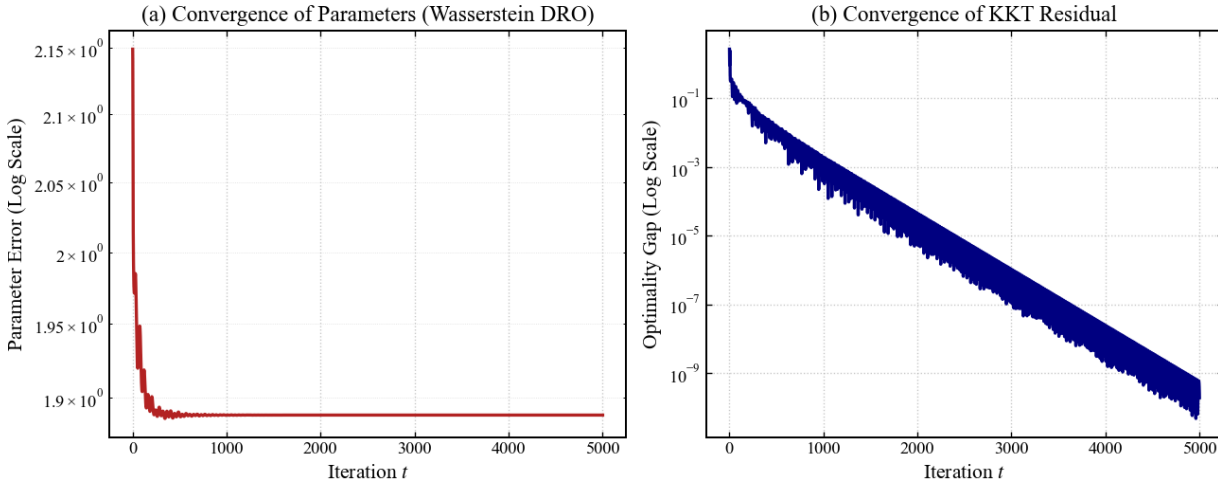


Figure 3: Convergence performance of the solution algorithm for the Wasserstein DRO estimator. Panel (a) illustrates the smooth stabilization of the parameter error. Panel (b) demonstrates the oscillated decrease of the KKT residual on a logarithmic scale over 5,000 iterations.

Figure 3 illustrates the convergence behavior of the Wasserstein DRO estimator. This numerical experiment is conducted in a data-scarce regime, featuring a 10-dimensional parameter space, 10 discrete alternatives, and a limited sample size of only 50 observations. The algorithm completes 5,000 iterations in just 1.26 seconds. Notably, the bilinear saddle-point formulation introduces the dual variable  $\gamma$  and the adversarial label distribution  $\mathbf{q}^\circ$ . The purely linear coupling of these variables can cause severe oscillatory “bang-bang” behavior and destabilize convergence under certain parameter configurations. To address this inherent instability in the min-max game, the algorithm effectively employs a two-time-scale strategy. By setting a larger step size for the inner maximization variables and performing multiple inner iterations per primal update, the adversarial distribution is forced to sufficiently approximate the local worst-case scenario.

## 5.2 Experiments on the Synthetic Dataset

To evaluate the finite-sample performance and robustness properties of the proposed estimators, we construct a synthetic experimental environment governed by certain PUM ground truths. The data generation process is specifically designed to simulate realistic decision-making scenarios characterized by inherent trade-offs rather than obvious dominance. For a set of  $m$  alternatives and  $k$  attributes, we first generate baseline feature vectors. Individual heterogeneity and measurement errors are introduced by superimposing independent Gaussian noise onto these baseline features for each of the  $N$  decision-makers. The choice outcomes  $y_n$  are sampled according to the probabilities

derived from the linear systematic utilities  $V_{ni} = \boldsymbol{\beta}^\top \mathbf{x}_{ni}$ . To rigorously stress-test the estimators, we deliberately focus on a *data-scarce, high-variance* regime (e.g.,  $N = 40$  with a low norm for the true parameters). This challenging setting serves to highlight the instability of standard Fenchel-Young estimation and demonstrate the stabilization effects of the Wasserstein-DRO framework. In the subsequent analysis, we operationalize the two limiting regimes of the DRO framework by denoting the hyperparameter for the  $\ell_2$ -regularized estimator as  $\lambda_{\text{reg}}$ , and the penalty parameter corresponding to the Hinge loss estimator as  $\lambda_{\text{flp}}$ .

### 5.2.1 The $\ell_2$ -Regularized Estimator

First, we evaluate the performance of the  $\ell_2$ -regularized Fenchel-Young estimator, which corresponds to the limiting regime of the Wasserstein robust framework where the label mismatch penalty  $\kappa \rightarrow \infty$ . We set the data generation process to follow a standard MNL specification. In our evaluation, we first evaluate the derived scaling law, and then benchmark the performance and sensitivities of the proposed estimator with standard Fenchel-Young estimator in terms of sample size, and finally evaluate the general performance of the two aforementioned estimators.

First, we validate the theoretical scaling law for the regularization parameter derived in Proposition 5. We propose the following empirical formula for the regularization coefficient:

$$\lambda_{\text{pred}} = 0.13 \frac{\sqrt{d/N}}{\|\boldsymbol{\beta}^*\|_2}. \quad (82)$$

In our experiment, to ensure robustness, we first generate 100 test cases by randomly varying the sample size  $N \in [20, 200]$ , the feature dimension  $d$ , and the signal strength  $\|\boldsymbol{\beta}^*\|_2$ . For each test case, to assess the efficacy of this heuristic, we performed an exhaustive line search for each generated instance to identify the ‘‘oracle’’ regularization parameter  $\lambda_{\text{opt}}$  that strictly minimizes the mean squared error (MSE), and the evaluation of MSE is done by Monte-Carlo estimation with 100,000 randomly generated problem instances.

Figure 4 compares the predicted parameters against the optimal ones found via line search. The scatter plot reveals a strong log-linear correlation, with data points clustering tightly along the  $y = x$  identity line. Quantitatively, utilizing this closed-form heuristic yields an estimator whose MSE is, on average, only approximately 23% higher than the theoretical minimum achievable by the oracle parameter. This confirms that the proposed scaling law provides a reliable, data-driven guideline for hyperparameter tuning, effectively capturing the optimal bias-variance trade-off without the need for computationally expensive cross-validation.

Next, we conduct a controlled Monte Carlo simulation to evaluate the finite-sample behavior of the estimators. We first conduct a controlled experiment to evaluate and benchmark the estimator’s performance sensitivity to sample size. Therefore, we fix the parameter vector and generate the data using  $\boldsymbol{\beta}^* = [1.0, 2.0, 0.5]^\top$ . We varied the sample size  $N$  from 20 to 200, and for each sample size, we conduct Monte-Carlo estimation with 100,000 randomly generated problem instances. The regularized estimator utilized the dynamic scaling law validated in the previous section.

The results, illustrated in Figure 5, demonstrate the superior predictive accuracy of the Wasserstein-robust framework. Crucially, the  $\ell_2$ -regularized estimator achieves a lower MSE than the original unregularized Fenchel-Young estimator across the entire range of sample sizes investigated ( $N \leq 200$ ). This performance gap is particularly pronounced in the limited-data regime, where the robust estimator significantly reduces estimation error by curbing the variance inherent to small samples. Notably, even as the sample size increases towards 200, the regularized estimator maintains a consistent advantage over the original model, indicating that the proposed scaling law effectively balances bias and variance without being overtaken by the unregularized MLE within this range.

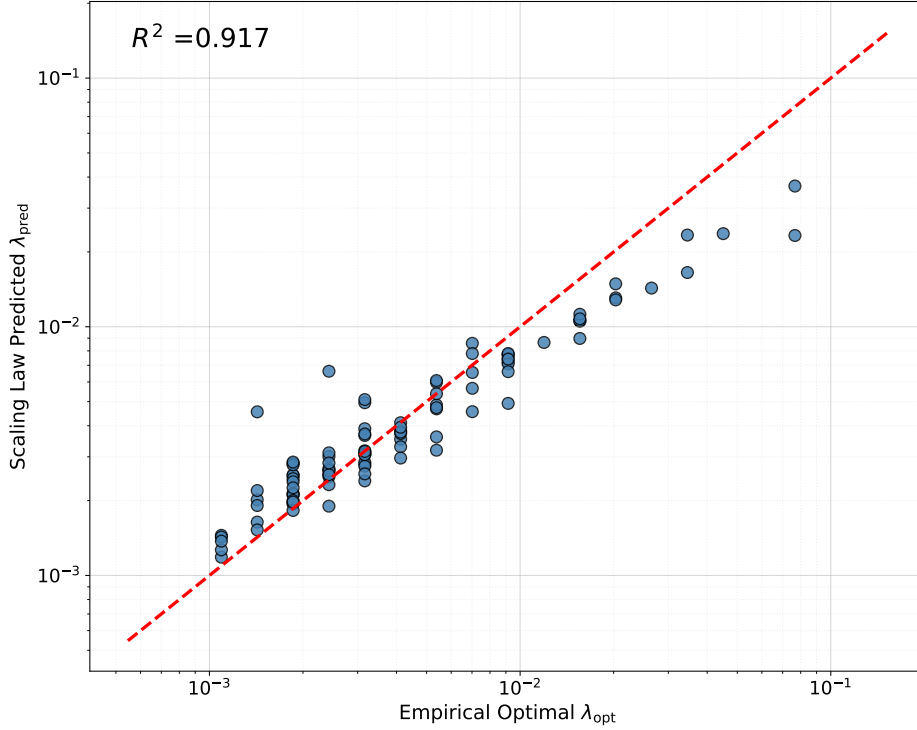


Figure 4: Validation of the regularization scaling law. The scatter plot compares the optimal regularization parameter  $\lambda$  obtained via exhaustive line search against the predicted value from the empirical formula. The strong alignment along the  $y = x$  line demonstrates that the formula  $\lambda_{\text{reg}} = 0.13 \frac{\sqrt{d/N}}{\|\beta^*\|_2}$  yields results that are highly consistent with the optimal parameters.

Next, we evaluate and benchmark the estimators' robustness to varying parameter scales by testing the model across a diverse range of  $\beta$  magnitudes. To this end, we first generate 1,000 set of parameters using  $\beta \in ([-5, 5]^3)$ , for each set of parameters, we vary the sample size from 20 to 200 and utilize Monte-Carlo experiment with 100,000 repetitions to obtain the estimator performance. The comparative performance of the proposed estimator is shown in Table 1,

Table 1: Robustness of the proposed  $\ell_2$  estimator to varying parameter scales. The reported win rate represents the percentage of tested parameters where the  $\ell_2$  estimator achieves a lower MSE. The Average MSE reduction indicates the average percentage of MSE reduced by the  $\ell_2$  estimator compared to the standard estimator. Overall, the  $\ell_2$  estimator is superior in all cases and can significantly reduce the MSE of the parameter estimates.

Sample size	Reg win rate	Average MSE reduction
20	100%	99.5%
60	100%	99.9%
100	100%	99.8%
140	100%	99.6%
180	100%	99.4%

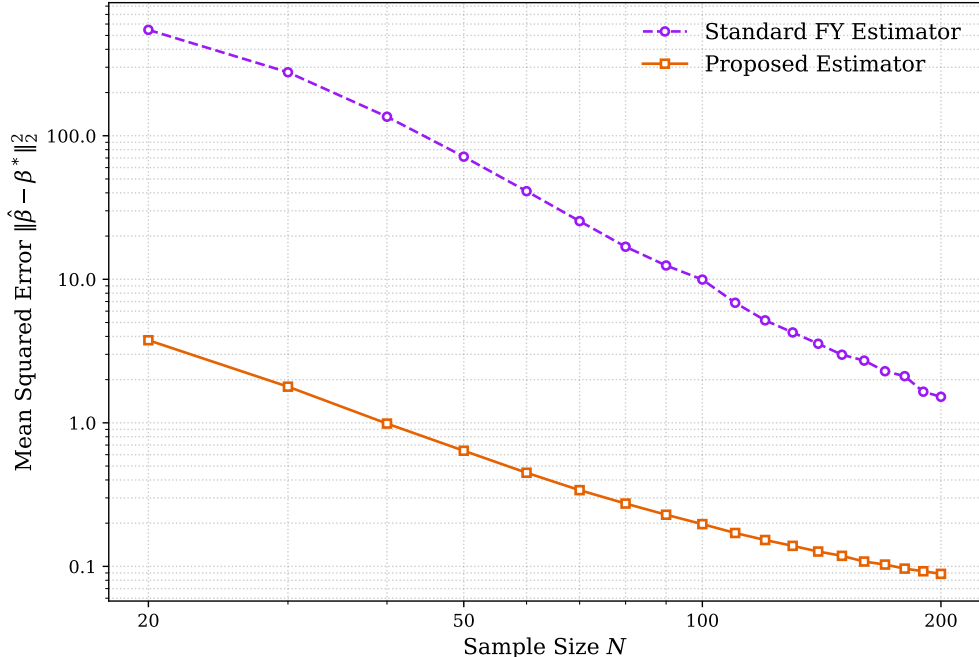


Figure 5: Comparison of MSE between the estimators. Notably, when the sample size is small ( $N \leq 200$ ), the  $\ell_2$  regularized Fenchel-Young estimator achieves a significantly lower average MSE compared to the original FY estimator, demonstrating better robustness in data-scarce regimes.

The results in Table 1 illustrate that the advantage of the  $\ell_2$  estimator is parameter-independent and consistent. In all sample sizes and parameters tested, the  $\ell_2$  estimator always outperforms the standard FY estimator, demonstrating its consistent advantage. Furthermore, the MSE reduction is consistent, as the  $\ell_2$  estimator is shown to be able to reduce the average MSE by over 99.4%.

### 5.2.2 The Hinge Loss Estimator

In parallel to the previous analysis, we now turn our attention to the pure margin-enforcing estimator. This corresponds to the regime where the parameter regularization is removed ( $\lambda_{\text{reg}} = 0$ ), and the distributional robustness relies entirely on the label mismatch penalty  $\lambda_{\text{flip}}$ . The experimental setup remains identical to that of the  $\ell_2$ -regularized estimator, covering a diverse range of sample sizes  $N$  and dimensions  $d$  under a MNL specification.

A key hypothesis of our framework is that the optimal safety margin should be inversely proportional to the statistical difficulty of the problem. We specifically test the empirical scaling law:

$$\lambda_{\text{pred}} = 2.9 \left( \frac{\sqrt{d/N}}{\|\beta^*\|_2} \right)^{-1}. \quad (83)$$

To validate this, we performed a grid search to determine the optimal  $\lambda_{\text{pred}}$  for each generated instance. The numerical experiment procedure is consistent with the setting and parameters of the scaling law validation in Section 5.2.1. As shown in Figure 6, there is a high degree of correlation between the optimal values and those predicted by the inverse formula. This strong alignment confirms that the proposed heuristic accurately captures the relationship between data sparsity and the necessary adversarial margin.

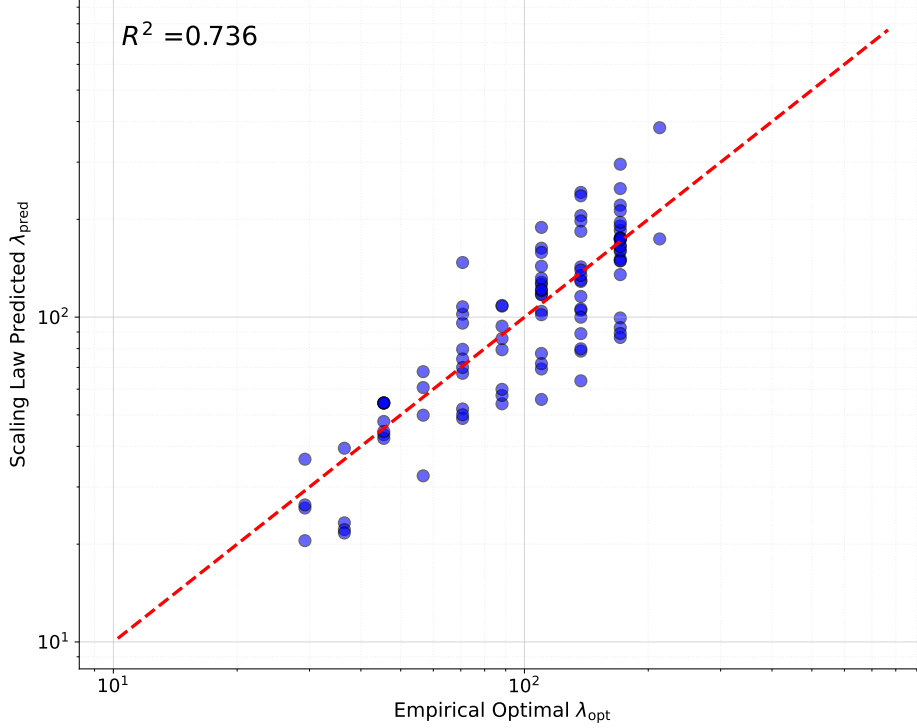


Figure 6: Validation of the Margin Scaling Law. This scatter plot compares the optimal label mismatch penalty  $\lambda_{\text{flp}}$  obtained via exhaustive grid search against the value predicted by the empirical inverse-complexity formula  $\lambda_{\text{pred}} \propto \left(\frac{\sqrt{d/N}}{\|\beta\|}\right)^{-1}$ . The tight clustering along the identity line ( $y = x$ ) confirms that the optimal safety margin is inversely proportional to the statistical difficulty of the problem.

Next, we benchmark the performance of the proposed Hinge estimator against the standard FY estimator. First, retaining the numerical experiment procedure in generating Figure 5, we evaluate the relative performance using  $\beta^* = [1.0, 2.0, 0.5]^\top$ . The corresponding MSE comparisons of the pure margin estimator are illustrated in Figure 7. Similar to the regularized case, the Hinge Loss estimator consistently achieves a significantly lower Mean Squared Error than the original unregularized Fenchel-Young estimator across the entire observed range ( $N \leq 200$ ). This confirms that enforcing an adversarial safety margin is a highly effective strategy for robustness, capable of suppressing estimation error even in the absence of explicit parameter shrinkage.

However, a notable distinction arises in the shape of the convergence trajectory. Unlike the smooth descent observed in the  $\ell_2$ -regularized model, the MSE of the Hinge Loss estimator does not decrease monotonically with the sample size. This fluctuation is likely attributable to the nature of the hyperparameter specification. While the scaling law for  $\lambda_{\text{reg}}$  is supported by a rigorous theoretical derivation based on asymptotic normality, the inverse scaling formula for  $\lambda_{\text{flp}}$  is primarily empirical. Consequently, the predicted margin may not be locally optimal for every specific sample size, leading to minor oscillations in performance despite the overall advantage in robustness.

Finally, we evaluate the robustness of the Hinge estimator towards ground truth parameter magnitude and shape. The numerical experiment procedure and parameter are the same as those of Table 1 in Section 5.2.1. The results are illustrated in Table 2.

Similar to the  $\ell_2$  estimator, the findings in Table 1 demonstrate that the Hinge estimator’s

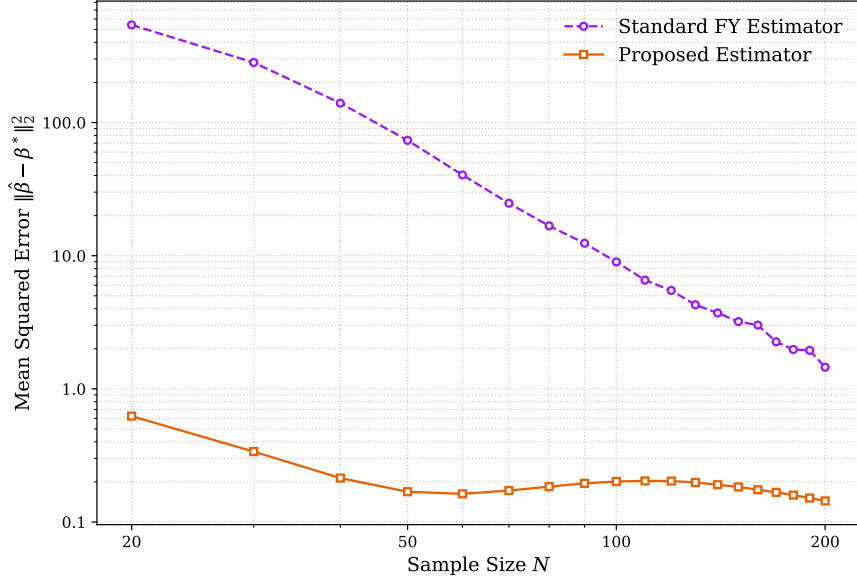


Figure 7: The figure illustrates the convergence of the MSE as the sample size  $N$  increases. The Wasserstein robust estimator (green solid line), configured with a pure adversarial margin ( $\lambda_{\text{reg}} = 0$ ), demonstrates superior performance in the small-sample regime ( $N \leq 200$ ) compared to the standard FY estimator (red dashed line).

Table 2: Robustness of the proposed Hinge estimator to varying parameter scales. The win rate indicates the frequency with which the Hinge estimator achieves a lower MSE, while the average MSE reduction measures its percentage improvement over the standard approach. In all cases, the Hinge estimator proves strictly superior, significantly diminishing the MSE of the parameter estimates.

Sample size	Hinge win rate	Average MSE reduction
20	100%	99.2%
60	100%	99.9%
100	100%	99.9%
140	100%	99.6%
180	100%	98.8%

superiority is both parameter-invariant and robust across different sample sizes. In every tested scenario, the Hinge estimator systematically outperforms the standard FY benchmark. This performance edge is remarkably stable, with the proposed method consistently reducing the average MSE by more than 98.8%.

### 5.2.3 Comparisons between Two Wasserstein Fenchel-Young Estimators

Having analyzed the two limiting regimes of the Wasserstein distributionally robust framework separately, we now turn to a direct comparison between the  $\ell_2$ -regularized estimator (corresponding to  $\kappa \rightarrow \infty$ ) and the Hinge Loss estimator (corresponding to  $\kappa, \epsilon \rightarrow 0$ ). To ensure the generality of our conclusions, we conducted extensive numerical experiments covering a wide grid of configurations,

varying the sample size  $N$ , the feature dimension  $k$ , and the signal strength  $\|\beta^*\|_2$ .

The results display a remarkably consistent pattern across virtually all tested scenarios. As exemplified in Figure 8, when both estimators are tuned to their respective optimal hyperparameters, the Hinge Loss estimator consistently yields a lower MSE than its  $\ell_2$ -regularized counterpart. This performance gap suggests that the topology of the ambiguity set defined by the label mismatch cost is often more aligned with the intrinsic geometry of discrete choice errors than the feature transport cost.

We attribute this phenomenon to the different mechanisms by which the two estimators induce robustness. The  $\ell_2$ -regularization imposes a global, isotropic shrinkage on the parameter vector, effectively reducing variance by biasing all estimates towards zero regardless of the specific data structure. In contrast, the Hinge Loss estimator operates via a more refined truncation mechanism. By enforcing an adversarial margin, it specifically robustifies the model against samples that are predicted with insufficient confidence, while preventing the model from becoming over-confident on “easy” samples. This acts as a selective regularization that adapts to the hardness of individual observations, offering a more precise trade-off between bias and variance than the blunt instrument of uniform norm contraction.

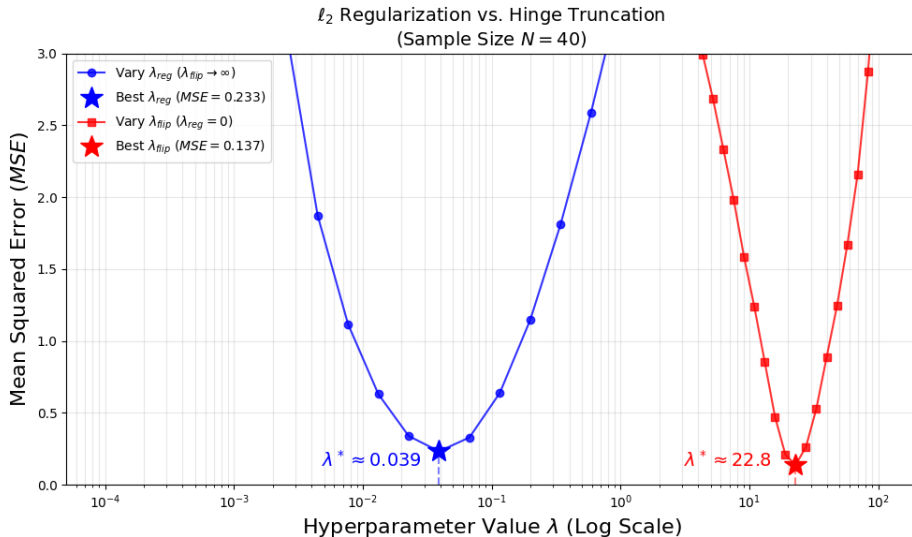


Figure 8: The figure illustrates one problem instance for testing the two robust estimators. It can be observed that the hinge loss estimator achieves smaller MSE at the optimal parameter.

### 5.2.4 Testing the Sparsemax PUM

In this final set of experiments, we extend our validation framework to the Sparsemax model. Unlike the Multinomial Logit model, Sparsemax induces sparse probability distributions where low-utility alternatives are assigned zero probability, providing a rigorous testbed for inherent data sparsity. First, to evaluate the small sample performance of the proposed estimators in the sparsemax case, we test the estimators on  $\beta^* = [1.0, 2.0, 0.5]^\top$ . Using this parameter, we vary the sample size from 20 to 200 and use Monte-Carlo experiment with 100,000 repetitions to estimate the MSE. We benchmark four distinct estimators: the Misspecified MLE (incorrectly assuming a Logit distribution), the Standard FY estimator (correctly specified but unregularized), and two Wasserstein-derived formulations—the Robust  $\ell_2$  estimator (utilizing dynamic regularization  $\lambda_{reg}$ )

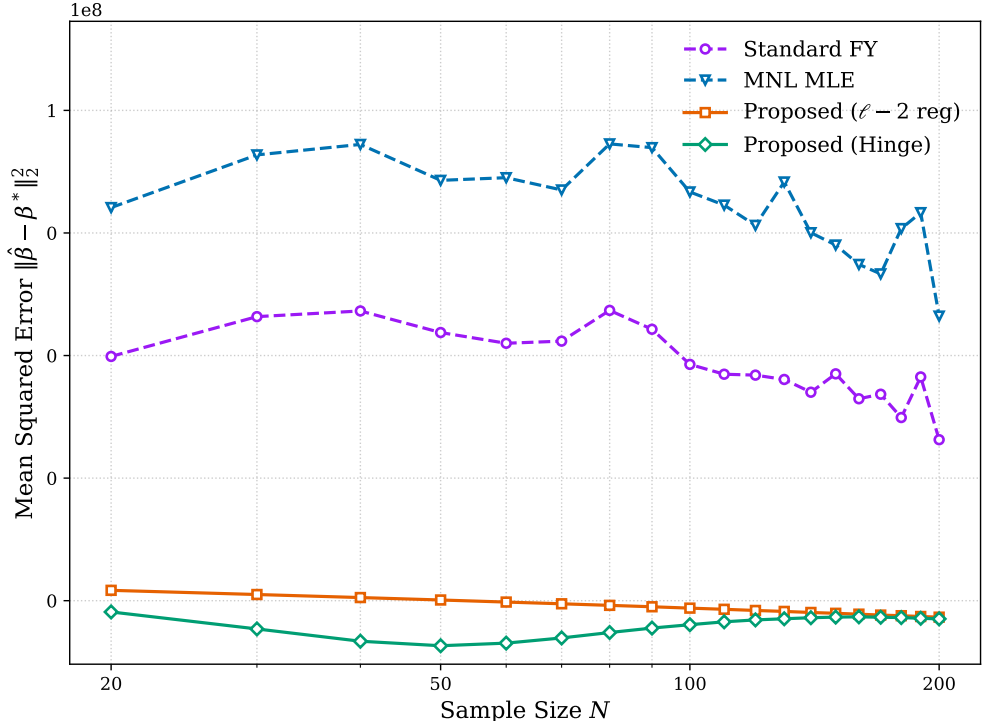


Figure 9: Comparisons among four different estimators for the Sparsemax instances.

and the Hinge Loss estimator (utilizing dynamic margin  $\lambda_{\text{flip}}$ ).

The comparative results are summarized in Figure 9. Three key observations emerge from this analysis. First, the Misspecified MLE consistently yields the worst performance across all instances. This confirms that forcing a dense probability model (Logit) onto sparse data introduces a severe structural bias that cannot be overcome by sample size alone.

Second, consistent with our MNL findings, both Wasserstein-derived robust estimators significantly outperform the standard unregularized FY estimator. The regularization effectively curbs the high variance associated with the non-smooth gradient transitions of the Sparsemax function in limited-data regimes.

Third, in the head-to-head comparison between the two robust formulations, the Hinge Loss estimator demonstrates superior adaptability. While both methods provide substantial improvements, the Hinge estimator achieves the lowest MSE in the majority of test cases. This suggests that the adversarial margin mechanism, which focuses regularization on the decision boundaries, is geometrically more compatible with the sparse support of the Sparsemax model than the isotropic parameter shrinkage imposed by the  $\ell_2$ -norm.

We also evaluate the robustness of the estimators in the sparsemax case by evaluating the performance using a set of different parameter  $\beta$ s. The results are shown in Table 3. On average, both robust estimators reduce the MSE by more than 99.9%.

### 5.3 Experiments on the Swissmetro Dataset

To validate the practical efficacy of the proposed estimators, we conduct an empirical study using the Swissmetro dataset, a canonical benchmark in discrete choice analysis (Bierlaire et al., 2001). Collected in 1998, this Stated Preference (SP) survey captures the decision-making behavior of

Table 3: Robustness of the proposed estimators to varying parameter scales in the sparsemax setting. The win rate denotes the frequency with which the corresponding estimator achieves a lower MSE than the standard FY estimator, while the average MSE reduction quantifies the mean improvement in estimation accuracy. These results demonstrate both estimators’ consistent superiority and their ability to significantly enhance parameter precision across all evaluated cases.

Sample size	Reg win rate	Reg MSE reduction	Hinge win rate	Hinge MSE reduction
20	100%	99.9%	100%	99.9%
60	100%	99.9%	100%	99.9%
100	100%	99.9%	100%	99.9%
140	100%	99.9%	100%	99.9%
180	100%	99.9%	100%	99.9%

commuters and business travelers along the St. Gallen-Geneva corridor. Respondents were presented with hypothetical choice situations involving three alternatives: private car, existing public train services, and the Swissmetro—a revolutionary underground mag-lev system operating at high speeds. The choices are driven by key attributes such as travel time, travel cost, and headway. By simulating data-scarce scenarios via subsampling from this real-world dataset, we rigorously evaluate the ability of our Wasserstein robust estimation framework to recover stable preference parameters and mitigate overfitting compared to standard Fenchel-Young estimators (MLE in the context of MNL).

In our experimental setup, we first pre-processed the raw data by retaining only observations where the car alternative was available and removing invalid choice indicators, ensuring a consistent choice set. The systematic utility functions are specified according to the standard model structure defined in Bierlaire et al. (2001), incorporating attributes such as travel time, cost, frequency, and season ticket ownership (GA) across three alternatives: Train, Swissmetro, and Car. To evaluate the estimators in a controlled data-scarce environment, we adopt a “population-proxy” approach where the parameters estimated from the full dataset serve as the ground truth (Oracle). We then conduct a Monte Carlo simulation by randomly subsampling datasets of size  $N$  ranging from 20 to 400. For each  $N$ , we average the performance metrics over 5,000 independent trials, comparing the standard unregularized estimator (MLE) against our two Wasserstein estimation formulations: the  $\ell_2$ -regularized estimator and the Hinge Loss estimator. Crucially, the regularization hyperparameters are determined directly via our scaling laws, thereby testing the validity of our derivation without relying on cross-validation.

The empirical results presented in Figure 10 provide compelling evidence for the superiority of the Wasserstein estimation framework in data-scarce regimes. As illustrated in Panel (b), there exists a dramatic divergence in estimator performance when the sample size  $N$  is small ( $N < 100$ ). The standard MLE (blue line) suffers from severe overfitting, exhibited by an estimation error gap exceeding  $10^4$  at  $N = 20$ . This empirically confirms the “curse of limited data” discussed in Section 4.1, where the unregularized estimator chases the idiosyncratic noise of the finite sample rather than capturing the structural preferences.

In sharp contrast, both Wasserstein-derived estimators maintain a tight proximity to the Oracle benchmark throughout the sampling range. The robustification significantly suppresses the variance, reducing the log-likelihood gap by nearly two orders of magnitude in the smallest samples. Notably, the Hinge Loss estimator (green triangle) demonstrates exceptional stability in the extreme low-sample limit, supporting the hypothesis that enforcing an adversarial margin is particularly effective

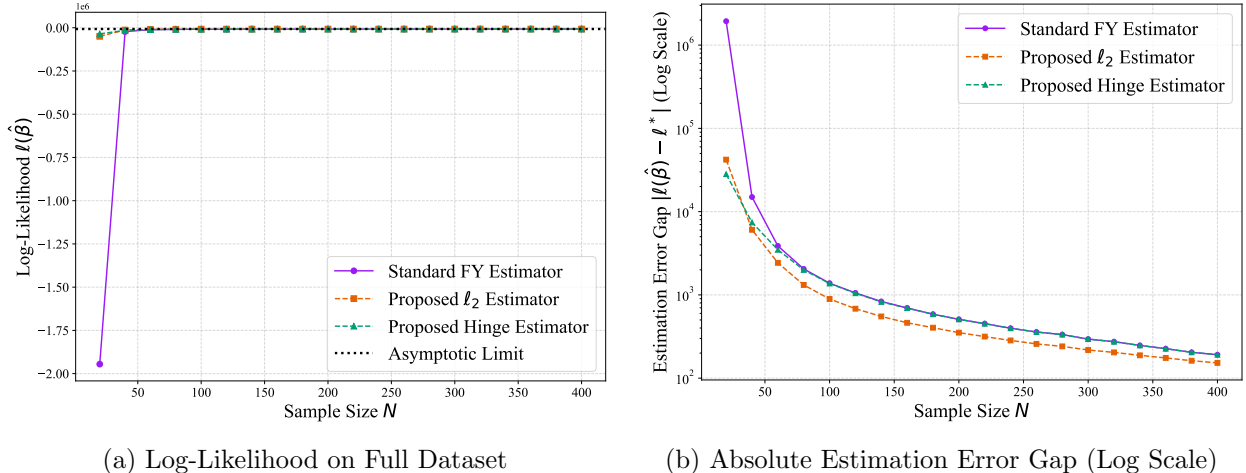


Figure 10: Performance comparisons on the Swissmetro dataset. **(a)** The evolution of Log-Likelihood on the full dataset as sample size  $N$  increases. **(b)** The absolute gap  $|\ell(\hat{\beta}) - \ell^*|$  relative to the Oracle estimator, plotted on a logarithmic scale. The Wasserstein FY estimators (both  $\ell_2$  and Hinge) demonstrate faster convergence and lower error in data-scarce regimes compared to MLE.

when data is insufficient to define a clear decision boundary. Furthermore, as  $N$  increases, all estimators show consistent convergence, yet the robust formulations consistently outperform the MLE. Most significantly, these performance gains were realized using the closed-form scaling laws derived in our theoretical analysis (e.g.,  $\lambda \propto \sqrt{d/N}$ ), without relying on computationally expensive cross-validation.

To rigorously assess the robustness of our framework under realistic survey conditions, we introduce a second experimental setup focusing on *decision-maker-based sampling* (ID sampling). Unlike the previous i.i.d. row sampling, this approach respects the panel structure of the Swissmetro dataset, where each respondent typically answers nine distinct choice situations involving micro-variations in attributes. We simulate data scarcity by randomly drawing  $K$  unique decision-makers, varying  $K$  from 6 to 40, and utilizing all associated choice observations for estimation.

The results, visualized in Figure 11, corroborate our earlier findings: the Wasserstein robust estimators (both  $\ell_2$  and Hinge) consistently outperform the standard MLE, maintaining a lower estimation error throughout the sampling range. However, two critical distinctions emerge when contrasting this cluster sampling with the previous random sampling regime.

First, despite comparable total observation counts, the log-likelihood gaps  $|\ell(\hat{\beta}) - \ell^*|$  for all three estimators are markedly higher in the ID sampling case. This phenomenon indicates that ID sampling exacerbates the negative effects of the small-sample regime. The high intra-personal correlation implies that the *effective* sample size is lower than the nominal observation count, making the empirical distribution significantly more sparse and prone to overfitting the idiosyncratic preferences of the few selected individuals.

Second, to counteract this intensified structural noise, the robust estimators required stronger regularization penalties. In this specific instance, the effective hyperparameters were scaled to  $\lambda_{\text{reg}} = 2$  and  $\lambda_{\text{flip}} = 0.03$ , values notably stronger than those required in the i.i.d. setting. This suggests that when data is not only scarce but also clustered, the “uncertainty radius” around the empirical distribution must be expanded, necessitating a more aggressive robustification strategy to recover stable population-level parameters.

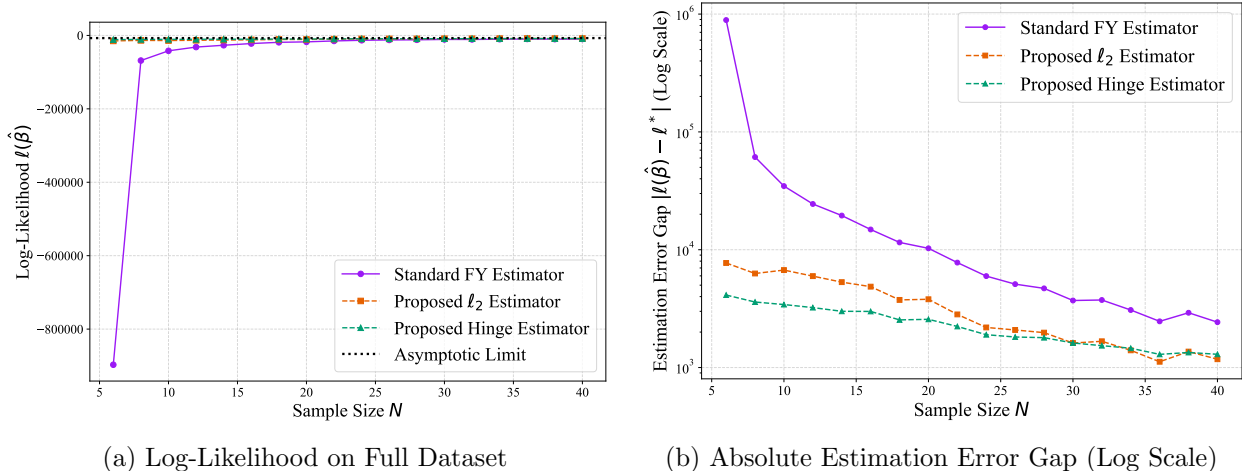


Figure 11: Performance comparisons on the Swissmetro dataset under decision-maker-based sampling. **(a)** The evolution of Log-Likelihood on the full dataset as the number of unique decision-makers  $K$  increases (ranging from 6 to 40). **(b)** The absolute gap  $|\ell(\hat{\beta}) - \ell^*|$  relative to the Oracle estimator, plotted on a logarithmic scale. The Wasserstein FY estimators (both  $\ell_2$  and Hinge) demonstrate superior stability and faster convergence compared to MLE.

## 6 Concluding Remarks

This paper establishes a unified, statistically robust estimation framework for Perturbed Utility Models (PUMs), offering a mathematically rigorous alternative to classical Maximum Likelihood Estimation (MLE). We highlighted the structural deficiencies of the traditional logarithmic scoring rule, specifically its susceptibility to non-convexity and numerical instability when evaluating modern, sparse choice architectures like the Sparsemax model. To resolve these fundamental pathologies, we introduced the Fenchel-Young estimator, which serves as a geometrically natural objective tailored to PUMs. By directly aligning the estimation loss with the convex conjugate structure of the choice probability mapping, the proposed Fenchel-Young estimator guarantees global convexity and bounded gradients, thereby securing computational stability even in strictly sparse regimes.

Furthermore, to overcome the pervasive challenge of data scarcity, we extended this framework through Wasserstein Distributionally Robust Optimization (DRO). This robust formulation explicitly incorporates distributional uncertainty surrounding the empirical data, successfully curtailing finite-sample bias and overfitting without compromising computational tractability. A central theoretical contribution of this extension is the rigorous unification of previously distinct regularization paradigms. Specifically, we proved that both standard  $\ell_2$ -regularization and the margin-enforcing Hinge loss naturally emerge as exact limiting cases of one tractable approximation of the Wasserstein-robust Fenchel-Young estimator.

Our theoretical claims were thoroughly validated through extensive numerical studies, encompassing both controlled synthetic environments and the empirical Swissmetro benchmark. Across these experiments, the proposed robust estimators consistently demonstrated superior performance over standard methodologies, recovering stable preferences in data-scarce and high-noise regimes where traditional estimators fail. Ultimately, this unified framework provides a cohesive, mathematically grounded toolkit for discrete choice analysis across transportation, economics, and marketing, ensuring reliable parameter inference even under severe data limitations and model sparsity.

Several promising directions for future research emerge from this work. First, our current

framework treats the perturbation function  $\Lambda$  as a fixed structural primitive (e.g., assuming a priori an entropic or quadratic form). A natural extension would be to incorporate the perturbation mechanism itself into the estimation process. Developing methods to jointly learn the systematic utility parameters and the shape of the choice kernel would allow for more flexible data-driven representations of decision-maker uncertainty and substitution patterns. Second, while this analysis focused on standard discrete choice scenarios with explicit choice sets, extending these robust estimators to more complex, structured domains is a critical frontier. In particular, applying the Wasserstein-Fenchel-Young framework to stochastic route choice problems, where the choice set comprises combinatorial paths in a network, presents unique challenges. Adapting the convexity results and dual reformulations to handle the recursive nature of such high-dimensional decision environments represents a fertile ground for future investigation.

## Acknowledgment

The work described in this paper was partly supported by research grants from the National Science Foundation (CMMI- 2233057).

## References

- Albert, A. and Anderson, J. A. (1984). On the existence of maximum likelihood estimates in logistic regression models. *Biometrika*, 71(1):1–10.
- Anderson, S. P., de Palma, A., and Thisse, J.-F. (1992). *Discrete Choice Theory of Product Differentiation*. MIT Press, Cambridge, MA.
- Ben-Akiva, M. E. and Lerman, S. R. (1985). *Discrete choice analysis: theory and application to travel demand*, volume 9. MIT press.
- Bierlaire, M., Axhausen, K., and Abay, G. (2001). The acceptance of modal innovation: The case of swissmetro. In *Swiss transport research conference*, volume 1.
- Blanchet, J. and Murthy, K. (2019). Quantifying distributional model risk via optimal transport. *Mathematics of Operations Research*, 44(2):565–600.
- Blondel, M., Martins, A., and Niculae, V. (2019). Learning classifiers with fenchel-young losses: Generalized entropies, margins, and algorithms. In *The 22nd International Conference on Artificial Intelligence and Statistics*, pages 606–615. PMLR.
- Blondel, M., Martins, A. F., and Niculae, V. (2020). Learning with fenchel-young losses. *Journal of Machine Learning Research*, 21(35):1–69.
- Clark, M. D., Determann, D., Petrou, S., Moro, D., and de Bekker-Grob, E. W. (2014). Discrete choice experiments in health economics: a review of the literature. *Pharmacoeconomics*, 32(9):883–902.
- Daganzo, C. F., Bouthelier, F., and Sheffi, Y. (1977). Multinomial probit and qualitative choice: A computationally efficient algorithm. *Transportation Science*, 11(4):338–358.
- Donoso, P. and de Grange, L. (2010). A microeconomic interpretation of the maximum entropy estimator of multinomial logit models and its equivalence to the maximum likelihood estimator. *Entropy*, 12(10):2077–2084.

- Firth, D. (1993). Bias reduction of maximum likelihood estimates. *Biometrika*, 80(1):27–38.
- Fosgerau, M., Paulsen, M., and Rasmussen, T. K. (2022). A perturbed utility route choice model. *Transportation Research Part C: Emerging Technologies*, 136:103514.
- Fudenberg, D., Iijima, R., and Strzalecki, T. (2015). Stochastic choice and revealed perturbed utility. *Econometrica*, 83(6):2371–2409.
- Gabaix, X. (2014). A sparsity-based model of bounded rationality. *The Quarterly Journal of Economics*, 129(4):1661–1710.
- Gao, R. and Kleywegt, A. (2023). Distributionally robust stochastic optimization with wasserstein distance. *Mathematics of Operations Research*, 48(2):603–655.
- Hausman, J. and McFadden, D. (1984). Specification tests for the multinomial logit model. *Econometrica: Journal of the econometric society*, pages 1219–1240.
- Hofbauer, J. and Sandholm, W. H. (2002). On the global convergence of stochastic fictitious play. *Econometrica*, 70(6):2265–2294.
- Kuhn, D., Esfahani, P. M., Nguyen, V. A., and Shafieezadeh-Abadeh, S. (2019). Wasserstein distributionally robust optimization: Theory and applications in machine learning. In *Operations research & management science in the age of analytics*, pages 130–166. Informa.
- Lin, T., Jin, C., and Jordan, M. I. (2025). Two-timescale gradient descent ascent algorithms for nonconvex minimax optimization. *Journal of Machine Learning Research*, 26(11):1–45.
- Malhotra, N. K. (1984). The use of linear logit models in marketing research. *Journal of Marketing research*, 21(1):20–31.
- Martins, A. and Astudillo, R. (2016). From softmax to sparsemax: A sparse model of attention and multi-label classification. In *International conference on machine learning*, pages 1614–1623. PMLR.
- McFadden, D. (1972). Conditional logit analysis of qualitative choice behavior.
- McFadden, D. (1974). The measurement of urban travel demand. *Journal of public economics*, 3(4):303–328.
- McFadden, D. (1981). Econometric models of probabilistic choice. *Structural Analysis of Discrete Data with Econometric Applications*, pages 198–272.
- McFadden, D. L. and Fosgerau, M. (2012). A theory of the perturbed consumer with general budgets. Technical report, National Bureau of Economic Research.
- Mohajerin Esfahani, P. and Kuhn, D. (2018). Data-driven distributionally robust optimization using the wasserstein metric: Performance guarantees and tractable reformulations. *Mathematical Programming*, 171(1):115–166.
- Mokhtari, A., Ozdaglar, A. E., and Pattathil, S. (2020). Convergence rate of  $o(1/k)$  for optimistic gradient and extragradient methods in smooth convex-concave saddle point problems. *SIAM Journal on Optimization*, 30(4):3230–3251.

- Nesterov, Y. (1983). A method of solving a convex programming problem with convergence rate  $O(1/k^2)$ . *Soviet Mathematics Doklady*, 27(2):372–376.
- Ray, P. (1973). Independence of irrelevant alternatives. *Econometrica: Journal of the Econometric Society*, pages 987–991.
- Sur, P. and Candès, E. J. (2019). A modern maximum-likelihood theory for high-dimensional logistic regression. *Proceedings of the National Academy of Sciences*, 116(29):14516–14525.
- Touchette, H. (2005). Legendre-fenchel transforms in a nutshell. URL <http://www.maths.qmul.ac.uk/ht/archive/lfth2.pdf>, page 25.
- Wald, A. (1949). Note on the consistency of the maximum likelihood estimate. *The Annals of Mathematical Statistics*, 20(4):595–601.
- Wen, C.-H. and Koppelman, F. S. (2001). The generalized nested logit model. *Transportation Research Part B: Methodological*, 35(7):627–641.
- Yao, R., Fosgerau, M., Paulsen, M., and Rasmussen, T. K. (2024). Perturbed utility stochastic traffic assignment. *Transportation Science*, 58(4):876–895.

## A Proofs

### A.1 Proof of Lemma 1

Fix  $(x, \mathbf{y})$ . Recall that for any PUM, the Fenchel–Young loss can be written as

$$\ell_{\text{FY}}(\boldsymbol{\beta}; x, \mathbf{y}) = \Omega(\mathbf{V}(x; \boldsymbol{\beta})) - \mathbf{y}^\top \mathbf{V}(x; \boldsymbol{\beta}),$$

where  $\mathbf{y} \in \{0, 1\}^K$  is the one-hot representation of the observed choice.

We first show that  $\Omega(\cdot)$  is continuous. By definition,

$$\Omega(\mathbf{V}) = \sup_{\mathbf{p} \in \Delta} \{\mathbf{p}^\top \mathbf{V} - \Lambda(\mathbf{p})\}.$$

For each fixed  $\mathbf{p} \in \Delta$ , the map  $\mathbf{V} \mapsto \mathbf{p}^\top \mathbf{V} - \Lambda(\mathbf{p})$  is affine (hence continuous) in  $\mathbf{V}$ . Since  $\Delta$  is compact and  $\Lambda$  is continuous on  $\Delta$ , the supremum over a compact set of continuous functions is continuous. Thus  $\Omega(\mathbf{V})$  is continuous in  $\mathbf{V}$ .

Because  $\mathbf{V}(x; \boldsymbol{\beta})$  is affine in  $\boldsymbol{\beta}$ , the composition  $\boldsymbol{\beta} \mapsto \Omega(\mathbf{V}(x; \boldsymbol{\beta}))$  is continuous. The second term  $\boldsymbol{\beta} \mapsto \mathbf{y}^\top \mathbf{V}(x; \boldsymbol{\beta})$  is linear in  $\mathbf{V}$  and thus continuous in  $\boldsymbol{\beta}$ . Therefore

$$\boldsymbol{\beta} \mapsto \ell_{\text{FY}}(\boldsymbol{\beta}; x, \mathbf{y}) = \Omega(\mathbf{V}(x; \boldsymbol{\beta})) - \mathbf{y}^\top \mathbf{V}(x; \boldsymbol{\beta})$$

is continuous on  $\mathcal{B}$  for every fixed  $(x, \mathbf{y})$ .

We now work on a compact parameter set  $\mathcal{B}$ . We first obtain a linear growth bound for  $\Omega(\mathbf{V})$ .

Since  $\Delta$  is compact and  $\Lambda$  is continuous on  $\Delta$ , there exists a finite constant  $c_\Lambda := \sup_{\mathbf{p} \in \Delta} |\Lambda(\mathbf{p})| < \infty$ . Then for any  $\mathbf{V} \in \mathbb{R}^K$ ,

$$\Omega(\mathbf{V}) = \sup_{\mathbf{p} \in \Delta} (\mathbf{p}^\top \mathbf{V} - \Lambda(\mathbf{p})) \leq \sup_{\mathbf{p} \in \Delta} \mathbf{p}^\top \mathbf{V} + c_\Lambda.$$

Because  $\mathbf{p} \in \Delta$  is a probability vector, we have  $\mathbf{p}^\top \mathbf{V} \leq \|\mathbf{V}\|_\infty$ , so

$$\Omega(\mathbf{V}) \leq \|\mathbf{V}\|_\infty + c_\Lambda.$$

Similarly, using  $\inf_{\mathbf{p} \in \Delta} \Lambda(\mathbf{p}) > -\infty$ , one obtains a matching lower bound, and thus

$$|\Omega(\mathbf{V})| \leq \|\mathbf{V}\|_\infty + C_0$$

for some finite constant  $C_0$  depending only on  $\Lambda$ .

Next, for each  $(x, \mathbf{y})$  and  $\boldsymbol{\beta} \in \mathcal{B}$ ,

$$\ell_{\text{FY}}(\boldsymbol{\beta}; x, \mathbf{y}) = \Omega(\mathbf{V}(x; \boldsymbol{\beta})) - \mathbf{y}^\top \mathbf{V}(x; \boldsymbol{\beta}),$$

so

$$|\ell_{\text{FY}}(\boldsymbol{\beta}; x, \mathbf{y})| \leq |\Omega(\mathbf{V}(x; \boldsymbol{\beta}))| + |\mathbf{y}^\top \mathbf{V}(x; \boldsymbol{\beta})|.$$

Since  $\mathbf{y}$  is a one-hot vector (and thus  $\mathbf{y} \in \Delta$ ), we have  $|\mathbf{y}^\top \mathbf{V}| \leq \|\mathbf{V}\|_\infty$ . Therefore:

$$|\ell_{\text{FY}}(\boldsymbol{\beta}; x, \mathbf{y})| \leq 2\|\mathbf{V}(x; \boldsymbol{\beta})\|_\infty + C_0.$$

Since  $\mathcal{B}$  is compact, there exists  $C_\beta > 0$  such that  $\|\boldsymbol{\beta}\| \leq C_\beta$  for all  $\boldsymbol{\beta} \in \mathcal{B}$ . Moreover, assuming each component of  $\mathbf{V}(x; \boldsymbol{\beta})$  is of the form  $V_i(x; \boldsymbol{\beta}) = \boldsymbol{\beta}^\top x_i$ , we have

$$\|\mathbf{V}(x; \boldsymbol{\beta})\|_\infty \leq \|\boldsymbol{\beta}\| \max_i \|x_i\| \leq C_\beta \max_i \|x_i\| \leq C_\beta \|x\|,$$

for a suitable norm  $\|\cdot\|$  on the feature space collecting all  $\{x_k\}$ . Thus we obtain

$$|\ell_{\text{FY}}(\boldsymbol{\beta}; x, \mathbf{y})| \leq C_1 \|x\| + C_2$$

for some finite constants  $C_1, C_2$  independent of  $\boldsymbol{\beta}$ , with  $C_1$  and  $C_2$  depending only on  $\mathcal{B}$  and  $\Lambda$ .

Define the envelope

$$M(x, \mathbf{y}) := C_1 \|x\| + C_2.$$

Under the standing moment condition that  $\mathbb{E}_{\mathbb{P}^*}[\|X\|] < \infty$ , we have  $M(X, \mathbf{Y})$  integrable. By construction,

$$|\ell_{\text{FY}}(\boldsymbol{\beta}; x, \mathbf{y})| \leq M(x, \mathbf{y})$$

for all  $\boldsymbol{\beta} \in \mathcal{B}$  and  $\mathbb{P}^*$ -almost all  $(x, \mathbf{y})$ . This proves the domination claim.

## A.2 Proof of Theorem 1

We split the proof into two main steps.

### Part 1: The population risk is uniquely minimized at $\boldsymbol{\beta}^*$ .

Recall the Fenchel–Young loss for a single observation  $(\mathbf{x}, \mathbf{y})$ :

$$\ell_{\text{FY}}(\boldsymbol{\beta}; \mathbf{x}, \mathbf{y}) = \Omega(\mathbf{V}(\mathbf{x}; \boldsymbol{\beta})) - \mathbf{y}^\top \mathbf{V}(\mathbf{x}; \boldsymbol{\beta}),$$

where  $\mathbf{V}(\mathbf{x}; \boldsymbol{\beta}) \in \mathbb{R}^K$  is the vector of systematic utilities and  $\mathbf{y} \in \{0, 1\}^K$  is the one-hot representation of the observed choice.

Denote the population (conditional) risk at covariate value  $\mathbf{x}$  by

$$\begin{aligned} L_{\mathbf{x}}(\boldsymbol{\beta}) &:= \mathbb{E}_{\mathbb{P}^*}[\ell_{\text{FY}}(\boldsymbol{\beta}; \mathbf{X}, \mathbf{Y}) \mid \mathbf{X} = \mathbf{x}] \\ &= \Omega(\mathbf{V}(\mathbf{x}; \boldsymbol{\beta})) - \mathbb{E}_{\mathbb{P}^*}[\mathbf{Y} \mid \mathbf{X} = \mathbf{x}]^\top \mathbf{V}(\mathbf{x}; \boldsymbol{\beta}). \end{aligned}$$

By the well-specified assumption, there exists a true parameter  $\boldsymbol{\beta}^*$  such that the conditional expectation of the observed choice matches the model probability:

$$\mathbb{E}_{\mathbb{P}^*}[\mathbf{Y} \mid \mathbf{X} = \mathbf{x}] = \mathbf{p}(\mathbf{x}; \boldsymbol{\beta}^*) \quad \text{for } \mathbb{P}^*\text{-a.e. } \mathbf{x},$$

where  $\mathbf{p}(\mathbf{x}; \boldsymbol{\beta}) = \nabla_{\mathbf{V}} \Omega(\mathbf{V}(\mathbf{x}; \boldsymbol{\beta}))$  is the choice probability vector predicted by the PUM.

Fix an  $\mathbf{x}$  in the support (we omit the  $\mathbf{x}$ -dependence in notation when clear). Let  $\mathbf{V} := \mathbf{V}(\mathbf{x}; \boldsymbol{\beta})$ ,  $\mathbf{V}^* := \mathbf{V}(\mathbf{x}; \boldsymbol{\beta}^*)$ , and  $\mathbf{p}^* := \mathbf{p}(\mathbf{x}; \boldsymbol{\beta}^*)$ . Then the conditional risk simplifies to:

$$L_{\mathbf{x}}(\boldsymbol{\beta}) = \Omega(\mathbf{V}) - (\mathbf{p}^*)^\top \mathbf{V}.$$

By the definition of the convex conjugate  $\Omega(\mathbf{V}) = \sup_{\mathbf{p} \in \Delta} \{\mathbf{p}^\top \mathbf{V} - \Lambda(\mathbf{p})\}$ , we have the Fenchel–Young inequality:

$$\Omega(\mathbf{V}) \geq (\mathbf{p}^*)^\top \mathbf{V} - \Lambda(\mathbf{p}^*), \quad \forall \mathbf{p}^* \in \Delta.$$

Rearranging this inequality yields a lower bound for the conditional risk:

$$L_{\mathbf{x}}(\boldsymbol{\beta}) = \Omega(\mathbf{V}) - (\mathbf{p}^*)^\top \mathbf{V} \geq -\Lambda(\mathbf{p}^*).$$

Now, evaluate the risk at the true parameter  $\boldsymbol{\beta}^*$ :

$$L_{\mathbf{x}}(\boldsymbol{\beta}^*) = \Omega(\mathbf{V}^*) - (\mathbf{p}^*)^\top \mathbf{V}^*.$$

From the properties of convex conjugates and the identity  $\mathbf{p}^* = \nabla\Omega(\mathbf{V}^*)$ , the supremum in the definition of  $\Omega$  is attained exactly at  $\mathbf{p}^*$ . Thus, the equality holds:

$$\Omega(\mathbf{V}^*) = (\mathbf{p}^*)^\top \mathbf{V}^* - \Lambda(\mathbf{p}^*),$$

which implies

$$L_{\mathbf{x}}(\boldsymbol{\beta}^*) = -\Lambda(\mathbf{p}^*).$$

Combining the inequality and the value at  $\boldsymbol{\beta}^*$ , we obtain:

$$L_{\mathbf{x}}(\boldsymbol{\beta}) \geq L_{\mathbf{x}}(\boldsymbol{\beta}^*) \quad \text{for } \mathbb{P}^*\text{-a.e. } \mathbf{x} \text{ and all } \boldsymbol{\beta} \in \mathcal{B}.$$

Moreover, equality  $L_{\mathbf{x}}(\boldsymbol{\beta}) = L_{\mathbf{x}}(\boldsymbol{\beta}^*)$  holds if and only if equality holds in the Fenchel–Young inequality. This occurs if and only if  $\mathbf{p}^*$  is a subgradient of  $\Omega$  at  $\mathbf{V}$ , i.e.,

$$\mathbf{p}^* = \nabla\Omega(\mathbf{V}) \implies \mathbf{p}(\mathbf{x}; \boldsymbol{\beta}^*) = \mathbf{p}(\mathbf{x}; \boldsymbol{\beta}).$$

Therefore, for  $\mathbb{P}^*$ -almost all  $\mathbf{x}$ ,

$$L_{\mathbf{x}}(\boldsymbol{\beta}) = L_{\mathbf{x}}(\boldsymbol{\beta}^*) \iff \mathbf{p}(\mathbf{x}; \boldsymbol{\beta}) = \mathbf{p}(\mathbf{x}; \boldsymbol{\beta}^*).$$

The total population risk is  $R(\boldsymbol{\beta}) := \mathbb{E}_{\mathbb{P}^*}[L_{\mathbf{X}}(\boldsymbol{\beta})]$ . Integrating the pointwise inequality implies  $R(\boldsymbol{\beta}) \geq R(\boldsymbol{\beta}^*)$ . Furthermore, if  $R(\boldsymbol{\beta}) = R(\boldsymbol{\beta}^*)$ , then  $L_{\mathbf{x}}(\boldsymbol{\beta}) = L_{\mathbf{x}}(\boldsymbol{\beta}^*)$  almost surely, which implies  $\mathbf{p}(\mathbf{x}; \boldsymbol{\beta}) = \mathbf{p}(\mathbf{x}; \boldsymbol{\beta}^*)$  almost surely. By the identifiability Lemma 2, this implies  $\boldsymbol{\beta} = \boldsymbol{\beta}^*$ . Thus,  $\boldsymbol{\beta}^*$  is the unique minimizer.

## Part 2: Uniform convergence and consistency.

Define the empirical FY risk as

$$R_N(\boldsymbol{\beta}) := \frac{1}{N} \sum_{n=1}^N \ell_{\text{FY}}(\boldsymbol{\beta}; \mathbf{X}_n, \mathbf{Y}_n).$$

By Lemma 1, the loss function is continuous on the compact set  $\mathcal{B}$  and dominated by an integrable envelope. These conditions are sufficient to invoke the Uniform Law of Large Numbers (see, e.g., Newey and McFadden, 1994, Lemma 2.4), yielding:

$$\sup_{\boldsymbol{\beta} \in \mathcal{B}} |R_N(\boldsymbol{\beta}) - R(\boldsymbol{\beta})| \xrightarrow{P} 0.$$

We now apply the standard consistency argument for extremum estimators. Fix  $\varepsilon > 0$ . Since  $\mathcal{B}$  is compact and  $\boldsymbol{\beta}^*$  is the unique minimizer of the continuous function  $R(\boldsymbol{\beta})$ , the minimum of  $R$  over the complement of the  $\varepsilon$ -ball is strictly separated from the global minimum:

$$\delta_\varepsilon := \inf_{\{\boldsymbol{\beta} \in \mathcal{B}: \|\boldsymbol{\beta} - \boldsymbol{\beta}^*\| \geq \varepsilon\}} R(\boldsymbol{\beta}) - R(\boldsymbol{\beta}^*) > 0.$$

Consider the event  $\{\|\hat{\boldsymbol{\beta}}_N - \boldsymbol{\beta}^*\| \geq \varepsilon\}$ . On this event, we have  $R(\hat{\boldsymbol{\beta}}_N) \geq R(\boldsymbol{\beta}^*) + \delta_\varepsilon$ . At the same time, by definition of the estimator,  $R_N(\hat{\boldsymbol{\beta}}_N) \leq R_N(\boldsymbol{\beta}^*)$ . We can bound the population risk difference:

$$\begin{aligned} R(\hat{\boldsymbol{\beta}}_N) - R(\boldsymbol{\beta}^*) &= (R(\hat{\boldsymbol{\beta}}_N) - R_N(\hat{\boldsymbol{\beta}}_N)) + (R_N(\hat{\boldsymbol{\beta}}_N) - R_N(\boldsymbol{\beta}^*)) + (R_N(\boldsymbol{\beta}^*) - R(\boldsymbol{\beta}^*)) \\ &\leq |R(\hat{\boldsymbol{\beta}}_N) - R_N(\hat{\boldsymbol{\beta}}_N)| + 0 + |R_N(\boldsymbol{\beta}^*) - R(\boldsymbol{\beta}^*)| \\ &\leq 2 \sup_{\boldsymbol{\beta} \in \mathcal{B}} |R_N(\boldsymbol{\beta}) - R(\boldsymbol{\beta})|. \end{aligned}$$

Combining these inequalities, the event  $\|\hat{\boldsymbol{\beta}}_N - \boldsymbol{\beta}^*\| \geq \varepsilon$  implies that  $2 \sup_{\boldsymbol{\beta}} |R_N - R| \geq \delta_\varepsilon$ . Therefore:

$$\mathbb{P}(\|\hat{\boldsymbol{\beta}}_N - \boldsymbol{\beta}^*\| \geq \varepsilon) \leq \mathbb{P}\left(\sup_{\boldsymbol{\beta} \in \mathcal{B}} |R_N(\boldsymbol{\beta}) - R(\boldsymbol{\beta})| \geq \frac{\delta_\varepsilon}{2}\right).$$

By uniform convergence, the probability on the right-hand side converges to 0 as  $N \rightarrow \infty$ . Thus,  $\hat{\boldsymbol{\beta}}_N \xrightarrow{p} \boldsymbol{\beta}^*$ .